JOURNAL OF MATERIALS SCIENCE 29 (1994) 614–631

Review
Nanocrystalline high melting point compound-based materials

R. A. ANDRIEVSKI
Institute for New Chemical Problems, Russian Academy of Sciences, Chernogolovka, Moscow Region, 142432, Russia

The different preparation methods of ultrafine powders of high melting point compounds (carbides, borides, nitrides, and oxides with melting temperatures higher than 2000 °C) are reviewed. Some properties of these powders are discussed and compared. The consolidation behaviour of these compounds in the nanocrystalline (nc) state is described in detail. Compaction by hot pressing, including high pressures and high temperatures, sintering, and high-energy consolidation methods, is analysed. The microstructure, recrystallization, mechanical and physical properties of nc-carbides, nitrides, and oxides are characterized. Special attention is focused on relationships between structure and properties.

1. Introduction

In recent years there has been increased interest in nanocrystalline (nc) (or nanostructured, nanophase or ultrafine grained) materials [1–4]. The development of nc materials is frequently connected with creating new generation materials. These materials are normally characterized by a grain size in the range 20–40 nm. It is generally accepted that the upper grain-size limit in nc materials is about 100 nm. Such small grain sizes are responsible for the unique physical and mechanical properties of shed bodies made from nc particulates. Extensive fundamental and applied investigations have been performed worldwide, for example in USA, Germany, Japan, Russia, UK, France, Ukraine, Latvia, and China.

In 1992, evaluations of progress in nc materials research and development was discussed at several specialized International meetings, including: the USA Materials Research Society 1992 Spring and Fall Meetings, "Nanophases and Nanocrystalline Structures" (1–5, March San-Diego, USA), "Nanophase and Nanocomposite Materials" (1–3, December Boston, USA); a NATO/ASI seminar on "Mechanical Properties and Deformation Behaviour of Materials Having Ultra-Fine Microstructures" (28 June–10 July 1992, Torres Vedras, Portugal); the "First International Conference on Nanostructured Materials" (21–26 September 1992, Cancun, Mexico); and the "Symposium on Nanophase Materials" (3–6 November 1992, Strasbourg, France). Nanophase materials research has also been reported at other venues, such as the 1992 Powder Metallurgy Congress in San Francisco, the American Institute of Chemical Engineers 1992 Annual Meeting, Miami Beach, etc. From 1992, the journal *Nanostructured materials* is being published in the USA.

Progress and development in nc materials studies have been reported in the recent reviews of Gleiter [1, 2], Siegel [3], Suryanarayana and Froes [4]. However, the problems of processing and the properties of high-melting point nc compounds (HMC) has not been fully surveyed to date. Included in this HMC category are carbides, nitrides, borides, oxides and other compounds with melting temperatures, (T_m), above 2000 °C (or even 2500 °C) [5, 6]. As shown by Andrievski and Spivak [6] two-component HMC systems number at least 130, with $T_m > 2500$ °C, with about 240 with $T_m > 2000$ °C. The number of the well-understood and practically used HMCs is considerably less. This review concentrates on nc HMCs that have been most extensively studied, such as Si_3N_4, SiC, TiN, TiC, TiB_2, WC, Al_2O_3, AlN, ZrO_2, MgO, Y_2O_3, BN and others. All these materials may be described as advanced ceramics. nc-TiO_2, nc aluminides of titanium and niobium are included in the study for comparison purposes.

This review is devoted to nc-materials in particulate form only. Thin films of nc materials by physical vapour deposition and chemical vapour deposition methods of film production and their properties, have been covered elsewhere (e.g. [7, 8]). In this review attention is focused on ultrafine powders (UFP) and their consolidation, and the properties of nc-materials.

2. Ultrafine powders

2.1. General characteristics

The problems concerning ultrafine powders (UFPs) have been known for many years in powder metallurgy, ceramics, catalysis, and other fields. It is common knowledge that UFPs have good sinterability and that some are characterized by high catalytic

0022–2461

TABLE I Methods of UFP preparation

Group	Method	Variation	Compound
Physical	Gas-condensation	In inert gas or vacuum	MgO, Al_2O_3, SiC [10–12]; Al_2O_3, Y_2O_3 [13]; ZrO_2 [14]
		In reactive gas	TiN, ZrN, NbN, AlN, VN, HfN [15, 16]; ZrO_2, Y_2O_3 [14, 17]
	High-energy destruction	Milling	ZrC [18]; Si_3N_4 [19, 20]; AlN, α-SiC [1, 21]
		Mechanical alloying	TiC, ZrC, TaC, WC, SiC [22–24]; TiB_2 [25]; TiN, BN, Si_3N_4, AlN, (Ti, AlN)N [26, 27]
		Detonative treatment	BN [28, 29]; Al_2O_3, MgO, SiC, TiC [30, 31]; Al_2O_3 [32]
Chemical	Synthesis	Plasma	TiN, ZrN, HfN, NbN, Ti(C, N) [33, 34]; AlN, BN, Si_3N_4, TiC, SiC, WC, Si_3N_4 + SiC [35–44]; TiN + TiB_2 [45]; Al_2O_3 [46]
		Laser	TiB_2 [47]; SiC [48]; Si_3N_4 [49]
		Thermal	BN, SiC [50–52]; WC–Co [53]; (Mo, W)$_2$C [54]; AlN [55]; ZrO_2 [56]; TiN + TiB_2 [57]
		Electrolysis	WC [58, 59]
		In solutions or liquids	Mo_2C, W_2C [60]; TiB_2, SiC [9, 61]
	Thermal decomposition	Condensive precursors	Si_3N_4, SiC, BN, AlN [9, 62–64]; ZrO_2, Y_2O_3 [62, 65, 66]; Si_3N_4 + SiC [67, 68]; NbN [69]
		Gaseous precursors	ZrB_{2+n} [70, 71]; BN [72]

activity and other unique properties. However, it is also well known that handling UFPs is difficult because of their poor technological properties, e.g. low values of apparent density and flow rate, high adsorbed gases and admixtures content, and poor compressibility at compaction, which are connected with the high surface area of UFPs and the influence of severe interparticle friction. The possibility of decreasing the sintering temperature is very attractive, but this advantage is still very remote for any practical application, and thus practical application of powders with particle size less than 100 nm (UFPs) is limited. However, the development of advanced ceramics has stimulated greatly the UFP preparation methods. Chemical synthesis routes to produce high surface-area non-oxide HMCs as applied to ceramics and catalysis, have been reviewed by Chorley and Lednor [9].

As with common powders, UFP preparation methods may be classified into physical and chemical groups, with some variants (see Table I). This classification is very conventional because in many cases the preparation method is based on more than one basic principle (e.g. gas-condensation technique in reactive atmospheres, mechanical alloying which is termed mechanosynthesis, etc.). It is generally supposed that the boundary between different powder preparation methods is often diffuse and poorly defined.

Some reviews of UFPs have recently been published (e.g. [9, 12, 62, 73, 74]) and therefore Table I does not include all results on HMC UFP but concentrates on the main and recent ones. From Table I it can be seen that many routes for UFP preparation exist which enlarges the technical possibilities but also creates the competition. However, in some cases these methods and their variations are mutually complementary.

2.2. Physical methods of preparation

2.2.1. Gas-condensation technique

Gas-phase condensation as a method for UFP preparation has long been known. Evaporation both into high vacuum and into inert or active gases applies to many metals, alloys and compounds, using a variety of heating sources (direct and indirect resistance, induction, electron beam, laser, electric arc, etc.). It is known that two prerequisites are necessary and sufficient for at least UFP condensation. The first is a high level of material vapour oversaturation, and the second is the presence in the condensed vapour of a neutral gas. The interpretation of gas-phase condensation phenomena, including homogeneous or heterogeneous nucleation, mechanism of particle growth, influence of impurities, etc., has been discussed elsewhere [12, 75].

The gas-condensation method for the preparation of nc materials has been improved significantly ([76, 77] and also [1–3]). As noted above, however, in all UFP preparation methods the most serious problem is in powder handling. Ensuring purity and high consolidation levels is not easy in UFPs. Attempts [76, 77] to generate and study bulk nc materials were based on a combination of the gas-condensation method and vacuum compaction, including the use of high pressures. This method has the advantage that UFP preparation and *in situ* collection, and compaction, are handled in a very clean environment.

A schematic representation of the inert gas-evaporation device is shown in Fig. 1 [3]. The material is evaporated from sources A and/or B into an inert-gas atmosphere (e.g., helium, about 1 kPa). The material vapour nucleates homogeneously owing to collisions with the cold inert gas atoms. The particle "fog" is transported by convection to the rotating liquid-nitrogen filled cold finger and condensed in the form of a loose UFP. This flaky powder layer is subsequently scraped from the finger, collected via the funnel and compacted first at low pressure device, and then at high pressure. The compaction pressure is up to 1–2 GPa (1–5 GPa [1]); the relative density of disc-shaped compacts (9–30 mm diameter, 0.1–1.0 mm thick) is about 0.7–0.9.

This apparatus is used for producing both nc metals

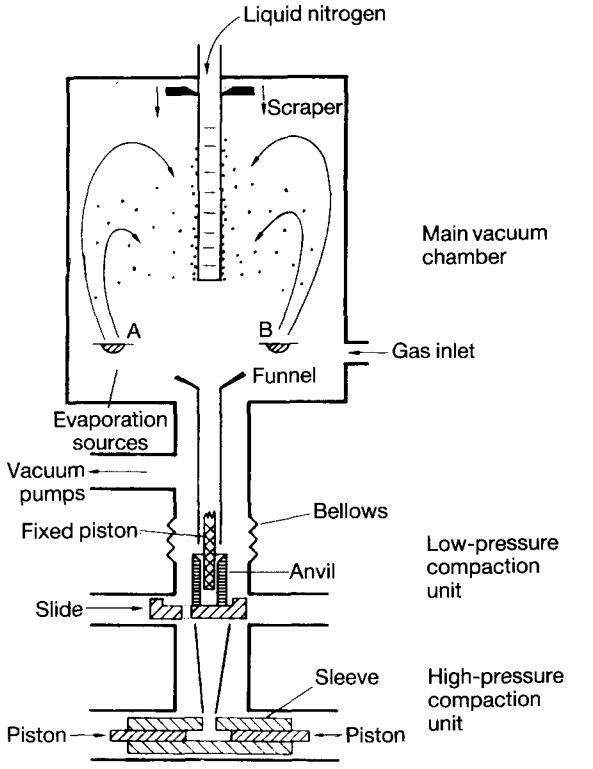

Figure 1 Schematic drawing of a gas-condensation chamber for nc material preparation [3].

and nc compounds (oxides, intermetallics etc.). Direct r.f. sputtering of an oxide and intermetallic target in an argon atmosphere and the reaction of a metal (titanium, zirconium) target in an $Ar-O_2$ atmosphere have been developed for the nc-TiAl, nc-TiO_2, and nc-ZrO_2 with average grain size from 11–30 nm [14, 78]. nc-Y_2O_3 was prepared by metal evaporation in helium gas (650 Pa pressure) with subsequent slow post-oxidation at 200 °C in 650 Pa of pure oxygen [17]. The Y_2O_3-particles obtained had a diameter, d, of $\sim$ 7 nm and were loosely aggregated. Unlike TiO_2 UFP, the Y_2O_3 UFP aggregates can be easily broken up. After compaction, these powders had a narrow pore-size distribution and were characterized by a high degree of transparency.

Another version of the inert gas-evaporation device, in which cooling is achieved by a refrigerated water–glycol mixture, has been described elsewhere [13].

Of the older works devoted to HMC UFP, a brief mention should be made of some Japan investigations. Iwama *et al.* [15, 16] have described the preparation of many UFP nitrides by evaporating source metals in low-pressure nitrogen or ammonia gas (130 Pa) using electron beam heating. UFPs thus prepared were found to have sizes ranging from 2–10 nm. Plasma flame, CO_2 laser beam and arc discharge heating techniques were used for MgO, Al_2O_3, SiC UFP preparation [10–12]. Other examples of the gas-condensation methods have been described by Gleiter [1] and Uyeda [12].

2.2.2. High-energy destruction

High-energy ball milling, including the popular attritor milling, is widely used for powder metallurgy and ceramics. There are some examples of its application for UFP preparation; however, there are at least two complications in its use. Firstly, it is known that the deceleration of powder size decreases after long milling times, even for brittle HMC (see, for example, [18]). Owing to this, the final size of the milled powders in many cases is not very small (about 100 nm). Secondly, the prevention of contamination is not easy to achieve. However, some information does exist concerning the successful use of cryomilling for the preparation of AlN UFP ($d < 50$ nm) [1] and turbomilling for the preparation of α-SiC ($d \sim 50$ nm) [21]. The attritor mill is used for wet grinding of Si_3N_4 powder [20]. The effect of milling time on the specific surface area, S, and the oxygen content is shown in Table II.

TABLE II The effect of milling time on specific surface area and oxygen content

	Initial	4 h	12 h
S ($m^2 g^{-1}$)	8.4	20	30 ($d \sim 60$ nm)
O_2 (wt %)	0.9	2.1	3.9

The company Netzsch Feinmahltechnik has developed a set of high-performance ceramic agitator mills in which the inner chamber, grinding disks and others are fabricated from oxide or non-oxide ceramics, depending on the product to be ground. This eliminates the contamination by iron and other metallic components, but not by oxygen.

In recent years, high-energy ball milling of elemental powders has gained acceptance in the preparation of UFP alloys and compounds. The synthesis of carbides, nitrides and borides by mechanical alloying is outlined in several investigations (e.g. [22–27]). Ogino *et al.* [27] described near-stoichiometric TiN formation after milling pure titanium for 40 h in a nitrogen atmosphere (ball-to-powder weight 13:1). It was observed by TEM that the milled powder particles had a diameter of about 5–7 nm. These small particles were then aggregated with larger ones (d = 0.1–0.27 μm). Chemical analysis indicated that after milling, contamination from the vial and balls occurred (about 8.8 at % Fe and 3.0 at %Cr).

Although, detonative treatment for the, activation of sintering and the synthesis of some HMC and diamond powders has long been known (see, for example, [28–32]), further systematic investigations of its application to nc HMC is required.

2.3. Chemical methods of preparation

2.3.1. Synthesis

These methods are considered to be the most universal for HMC preparation. The plasma-chemical synthesis of UFP is very popular. Comprehensive investigations of this process have been conducted in the former USSR (Russia [33, 34], Latvia [35–37], and Ukraine [38, 39]), in Japan [12] and other countries [9, 73, 74]. The low-temperature plasma provides a method for synthesis at the very high temperatures

(up to 6×10^4–8×10^4 K) that are responsible for the high levels of the oversaturation, chemical reaction and UFP condensation rates. The principal of the possibility of attaining an essentially all-HMC UFP preparation has been demonstrated by plasma treatment. Some typical UFP (d = 5–100 nm) produced by plasma synthesis are shown in Table I. The different variants of plasma reactors are used for UFP production : a direct-current (d.c.) arc jet [35–40, 42, 44–46], a radio frequency (r.f.) plasma device [33, 34, 41], and a hybrid one [43]. The d.c. plasma is considered to be more available, but the r.f. plasma device one may provide the more desired results. Kijima *et al.* [41] reported the synthesis by r.f. plasma of ultrapure SiC UFP (99.999% purity only for cation impurities; d = 5–20 nm).

It is also important for plasma technology to be used for the preparation of multi-component HMCs such as Si_3N_4 + SiC, Ti(N, C), Nb(N, C), TiN + TiB_2, Si_3N_4 + TiN(MgO, Y_2O_3, Al_2O_3), etc., and not just two component compounds.

Some information has been reported on the CO_2 laser synthesis of HMC UFP, but this continues to be studied intensively (e.g. [47–49]); however, data on the various properties of these powders are rather limited.

Our definition of "thermal synthesis" includes many different processes: carbothermal oxide reduction [50–52], direct solid-state synthesis [54] and thermolysis of chlorides in an NO_2 atmosphere [56], decarbonization treatment of the $AlCl_3$ + glucose mixture in NH_3 gas [55], and synthesis of titanium with boron–nitrogen polymer [57], as does hydrothermal synthesis [79]. An interesting new thermochemical method for the synthesis WC–Co UFP has been developed by McCandlish *et al.* [53], which includes the use of a precursor compound, $Co(en)_3WO_4$, in which tungsten and cobalt are intimately mixed at the molecular level; subsequent reduction and carburization yields WC–23 wt % Co. Other compositions of hard alloys may also be prepared. This technology yields a tungsten carbide grain size of about 200 nm in sintered hard alloys.

Other examples of chemical synthesis of UFPs as in the sol–gel process, are worth consideration. Non-oxide HMC can be synthesized by processing organometallic precursors (alkoxysilane, etc.). Hatakeyama and Kanzaki [80] described the synthesis of monodispersed spherical β-SiC powder derived from the hydrolysis of a mixture of phenyltriethoxysilane and tetraethyl orthosilicate. The SiC content in this powder is 92.6 wt % after heat treatment at 1500 °C for 4 h in an argon atmosphere; the spherical particles are 0.6 μm in diameter and consist of primary particles of about 40 nm diameter, as shown in Fig. 2. The possibilities of the sol–gel technology are considered to be important for the significant improvement of UFP technological properties. Recent developments of sol–gel technology are reviewed elsewhere [81].

Electrochemical synthesis of WC UFP (S = 5–10 $m^2 g^{-1}$) has been carried out in chloride melts at 700–750 °C [58, 59].

There is little comprehensive information on low-temperature wet-chemical synthesis. Alexbaum *et al.* [61] obtained TiB_2 UFP by precipitation from the solution-phase reaction of $TiCl_4$ and $NaBH_4$ and subsequent annealing to achieve crystallization at 850–1100 °C. Room-temperature synthesis of Mo_2C

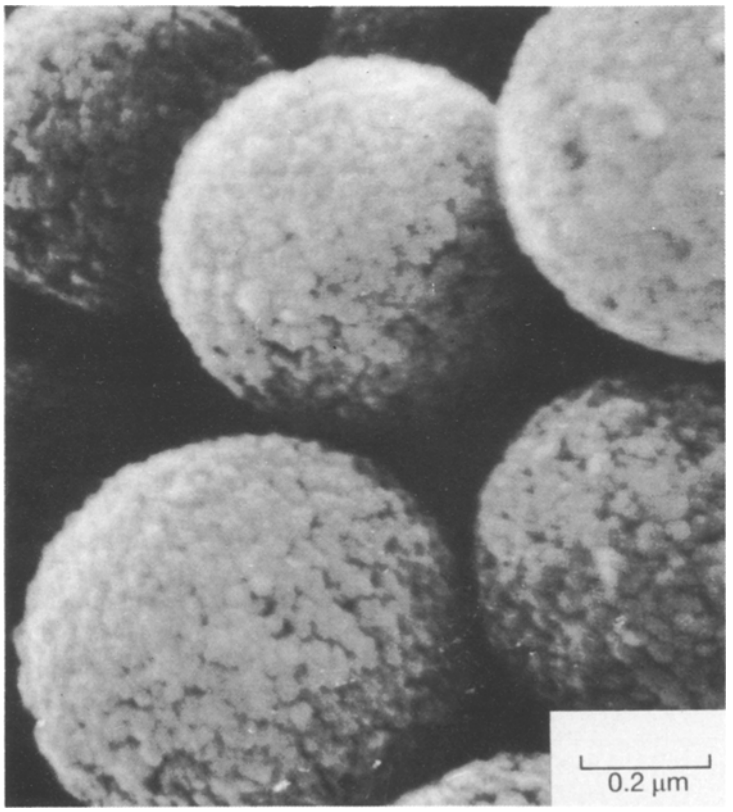

Figure 2 Microstructure of monodispersed spherical β-SiC [80].

and W_2C UFP (2 nm sized particles which agglomerates to 1–2 μm) by the reduction and carbidization of chlorides has also been described [60].

2.3.2. Thermal decomposition

Many HMC UFPs may be prepared by the thermal decomposition (thermolysis, pyrolysis, calcination) of solid, liquid and gaseous precursors. Different precursors as starting materials for oxide and non-oxide advanced ceramics have been reviewed [62]. As in the case of synthesis, sol–gel technology, cryochemical methods with sublimation drying of solutions, plasma, laser heating and many traditional technological methods are used.

Organometallic precursors are very important in the production of Si_3N_4 and SiC UFP. The decomposition of diimide Si $(NH)_2$ at a temperature above 1250 °C leads to the formation of high pure fine nitride powders which may be milled [63]. These technologies are used in industry, (Ube Ind., Japan and H. S. Starck, Germany). The pyrolysis of polycarbosilanes yields β-SiC UFP, 2–100 nm in size, depending on the pyrolysis temperature [63]. Gonsalves *et al.* [68] proposed a method for the ultra-rapid conversion of a liquid organosilazane $(CH_3SiHNH)_x$ using a CO_2 laser, to Si_3N_4 + SiC UFP.

In recent years, a marked interest has been taken in boride UFP. The very volatile group IV borohydrides, $Ti(BH_4)_4$, $Zr(BH_4)_4$, $Hf(BH_4)_4$, are very attractive molecular precursors for film and UFP preparation. These compounds may be decomposed at 300–400 °C. Zirconium boride UFP synthesis was attempted using both a CO_2 laser [70] and normal heating [71].

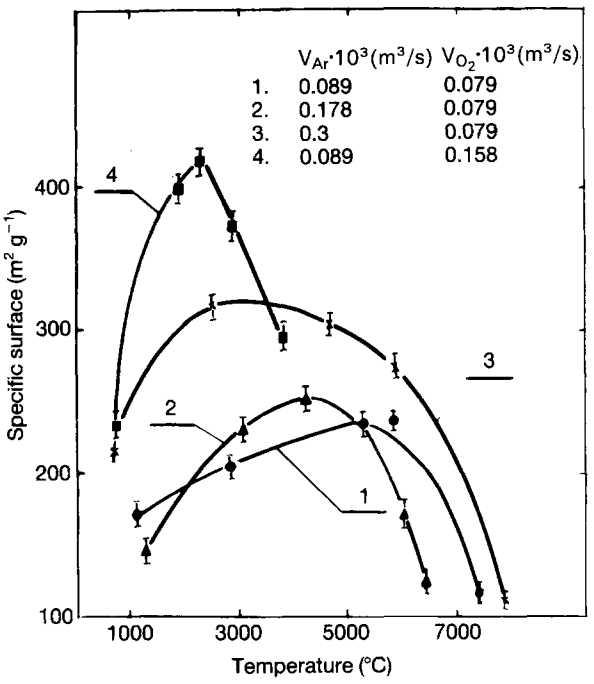

Figure 3 Al_2O_3 specific surface versus plasma temperature for different flow rates of plasma-forming gases, V_i, at an aluminium consumption of 24 g h^{-1} [46].

2.4. Properties of UFPs

2.4.1. Particle size, morphology and structure

The particle size of a UFP is its most important characteristic. The preparation conditions may have a pronounced effect on the particle size: Fig. 3 shows the effect of plasma temperature and flow rates of the plasma-forming gases on specific surface (S) for Al_2O_3 UFP [47]. A wide range of S is evident. In most cases it is necessary to prepare UFP with a narrow size distribution, and to achieve this, gas-condensation methods are generally considered to give more accurate results than chemical methods.

The particle size and morphology are studied by TEM. It is common knowledge that some medium-size values may be obtained in the study of S and by XRD-analysis of line-broadening determinations. Using the equation

$$S = 6/\gamma_{th} d_S \qquad (1)$$

where γ_{th} is the theoretical density, and d_S is the mean diameter defined from the S measurements, we can estimate the medium size values. Table III gives the values estimated for some HMC UFPs. It is clear from Table III that the variations in S for different UFPs with identical d_S vary by up to six or more times because of the difference in γ_{th}. It should be noted that in most cases, γ_{th} must be defined more exactly for any specific UFP, because of the effect of admixtures and defects.

In some cases, measured values of d show considerable variation between TEM method and S and XRD-analysis determinations. This may be due to the influence of morphology, particle-size distribution, degree of agglomeration and polycrystallinity. Kravchik and Neshpor [82] pointed out that values of d determined by S and XRD methods coincide for TiN UFP only at the S intervals greater than 30 m^2 g^{-1}

TABLE III Specific surface area values for some HMC UFPs (γ_{th} in parentheses)

d_S (nm)	S(m^2 g^{-1})					
	B_4C, BN (2.3–2.5 g cm^{-3})	Si_3N_4, SiC, MgO, AlN (3.3–3.4 g cm^{-3})	Al_2O_3, TiO_2, TiB_2, TiC (4–4.9 g cm^{-3})	TiN, Y_2O_3, (5.4–5.7 g cm^{-3})	NbN (8.3 g cm^{-3})	WC (15.8 g cm^{-3})
100	24–26	18–19	12–25	10–11	7	4
50	48–52	36–38	24–50	20–22	14	8
10	240–260	180–190	120–250	100–110	70	40

($d < 30$ nm) [82]. Petrunin *et al.* [83] also observed that the agreement between d values determined by TEM, S and neutron diffraction methods is good, for ZrN UFP with $d \sim 20$ nm [83]. However, for other sizes, the coincidence was poor. For ZrO_2 UFPs ($d = 8-20$ nm), the values of d determined from TEM and neutron diffraction studies was found to be totally satisfactory [84]. Almost without exception, therefore, several different methods should be used to enable comparison to be made.

Some results of the study of UFP morphology have been published [12, 15, 16, 38, 85–88]. The results of a study of Al_2O_3 and SiC UFP using high-resolution electron microscopy have been reviewed by Uyeda [12]. Polyhedral forms of UFPs were observed in studies of TaC, TiC, NbC and TaN UFPs obtained in d.c. plasma from chlorides and methane (or nitrogen) gases [85]. Some truly spherical particles, especially in the case of NbC and TaC, have also been observed. The regular grain-shaped form of particles has been found experimentally in TiN (Fig. 4), ZrN and VN UFPs obtained by plasma methods [86], whereas Aivazov *et al.* [87] have also observed the cubic-grained forms for γ–Al_2O_3 and $TiC_{0.95}$ and the hexahedral form for TiB_2. However, clear crystal habits are hardly observable in all the nitride particles which have been produced by evaporating source metals in low pressure nitrogen or ammonia gases [15, 16]. The spherical morphology is considered to be more frequent for niobium nitride obtained by plasma synthesis [86]. Changes of ammonia concentration in the plasma influences the production of spherical or polygonal AlN UFPs [38]. Amorphous UFPs, of course, have no granular forms. The shape of ball-milled UFP is irregular, and electrochemically synthesized WC UFPs exhibit different morphological forms [59]. It is worth noting that during UFP preparation, oxidation may influence the particle shape.

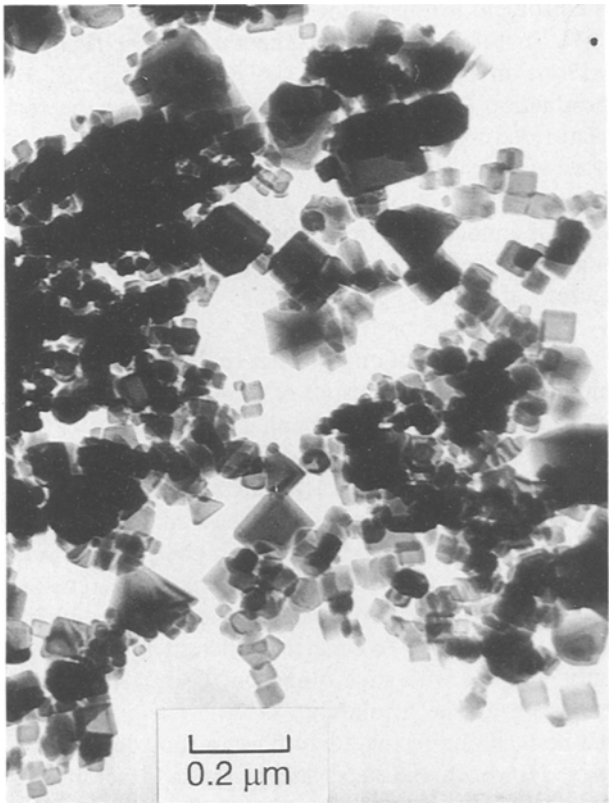

Figure 4 Electron micrograph of TiN.

It has been pointed out [75] that a study of the particle-size distribution curves may elucidate the UFP condensation mechanism. When there is a log-normal (Gaussian) distribution of particles, the most likely growth mechanism is a coagulation stage with participation of a liquid state. When deviation from the theoretical log-normal distribution occurs, growth through the vapour–crystal mechanism may predominate : the former example has been proved for spherical tungsten UFPs and the latter has been observed for polyhedral TiN UFP [75, 88]. However, both a log-normal distribution and regular polyhedron forms of some UFPs (TiC, TaC, NbC and TaN) have been observed by Neuerschwander [85].

Particular attention has been paid to the study of UFP structure by XRD and neutronography. Unfortunately, a detailed discussion of this problem cannot be made here because of space. Nevertheless, it is necessary to point out, four interesting features of UFP structure:

1. the availability of amorphous structures (e.g. Si_3N_4, Al_2O_3, SiC [13, 42, 49, 64];
2. the presence of anomalous structures (e.g. Al_2O_3, ZrO_2 [75, 84]);
3. the influence of d on the lattice parameter [83, 89, 90]; and
4. the absence of dislocations in small particles [75, 82].

These features are connected with the characteristic small sizes of UFPs and their preparation conditions (short chemical reaction times, high cooling rate values, influence of admixtures, etc.). Table IV shows the variation of structural parameters of TiN UFP. It is obvious that with decreasing d_S, the lattice parameter also decreases and the root mean square shift of atoms increases. This may be associated with the influence of a capillary compression and the presence

TABLE IV Structural parameters of TiN UFP [90]

Phase	S ($m^2 g^{-1}$)	d_S (nm)	Lattice parameter (nm)	Root mean square atom shift (nm)
$TiN_{0.96\pm0.02}$	39	27	0.424 02 ± 0.000 08	0.0098 ± 0.0007
$TiN_{1\pm0.05}$	50.3	22	0.423 81 ± 0.000 08	0.0100 ± 0.0020
$TiN_{0.98\pm0.03}$	53.2	21	0.423 84 ± 0.000 09	0.0080 ± 0.0020
$TiN_{0.87\pm0.08}$	76.4	14	0.423 71 ± 0.000 10	0.0100 ± 0.0010
$TiN_{0.98\pm0.04}$	83.5	13	0.423 67 ± 0.000 11	0.0101 ± 0.0005
$TiN_{0.96\pm0.04}$	95.4	11	0.423 54 ± 0.000 14	0.0131 ± 0.0002

TABLE V Some characteristics of Si_3N_4 powder [91]

Synthesis method	S ($m^2 g^{-1}$)	d_s (nm)	Particle shape	Crystallinity (%)	Content (wt %)		
					Oxygen	Carbon	Metallic impurities
Plasma-derived SiH_4/NH_3	6.5	260	Equiaxed	30	2.1	0.11	0.0106
CO_2 laser derived SiH_4/NH_3	120	17	Spherical	0	0.1–6	0.07	< 0.02
Flat flame reactor $SiH_4/NH_3/N_2H_4$	90–150	10–50	Equiaxed	0	~ 3		< 0.01

of heterogeneous deformations in small particles. The same situation has been described for ZrN UFPs [83]. However, TEM study of TiN UFP has not revealed the presence of dislocations [82].

2.4.2. Impurities and gas content

In most cases the admixture content in UFP is not very low compared with ordinary powders and especially with single crystals. This is connected with synthesis conditions and high values of S. However, as suggested earlier, the possibility of obtaining very pure β-SiC UFP has been reported [41]. It is very likely that only the conditions of the special gas-condensation technique (see Fig. 1) are able to prevent oxygen contamination. This method, though, is not universally applicable to all HMC UFPs, and it is necessary to analyse different powders. The various chemical contents are illustrated using Si_3N_4 UFPs as an example in Table V.

Si_3N_4 powder purity plays an important role in HIP behaviour and high-temperature strength, and thus the serious attention must be focused on handling and gas evaluation. Essentially all types of UFPs are characterized by a high content of adsorbed and chemisorbed gases [92], the main components being CO, CO_2, H_2, N_2, and H_2O, as has been demonstrated for Si_3N_4 and TiN UFPs during vacuum heating [93, 94]. The total volume, V, of escaped gases for different TiN powders is shown in Table VI. It follows that the gas content increases with increasing S. Detailed investigations of chemical and other properties of nitride UFPs were made by Troitskiy and coworkers [86, 95], who revealed that oxygen in these powders can be present both in the nitride solution and in the oxynitride films, and in the adsorbed gases state. Interesting information on the segregation of carbon, oxygen, and other elements, on the UFP surface, has been provided by XPS and AES methods (e.g. [96–98]).

TABLE VI Volume of escaped gas

	S ($m^2 g^{-1}$)		
	0.15	16	62
d_s (nm)	8×10^3	70	18
V ($cm^3 g^{-1}$)	1	7	33

2.5. Concluding remarks

The foregoing discussion does not exhaust the problems of UFP preparation and properties, only some aspects being discussed. Small particles ($d < 10$ nm) also have an independent importance and are worthy of separate consideration (see, for instance, [75, 99]). However, it is profitable to consider in brief the UFP preparation methods as a whole. Essentially many of them are used only on a laboratory or, at best, a pilot scale. The comparison of different UFP preparation methods is not easy because of limited information: the problem is only in the early stage of investigation [91]. In this connection, Schoenung's results are of interest in an analysis of the economics of Si_3N_4 production [100]. A large disparity between the cost of nitrided/milled powder ($d \sim 170$ nm) and the cost of laser-synthesized powder ($d \sim 17$ nm) has been revealed: about 30 and 115 $\$ kg^{-1}$, respectively (the latter is connected with the high cost of silane). At that time, however, the chemical impurities differed by a factor of two (~ 4 wt % for first powder and ~ 2 wt % for second).

The true value of any powder and any preparation method is defined by results of very careful processing, its economy and ecology, and the properties of not only the powders but also materials based on them. To date, in most cases, such plausible information is not available. Nevertheless, it is believed that the yield of the chemical methods may be higher than that of the physical ones. At the same time, as suggested earlier, there is no universal method for producing UFPs. From time to time the different methods not only compete with each other, but also may be complementary. The availability of different preparation methods is one of the advantages of powder technology. However, the need still exists to develop economical methods to produce large quantities of UFP with predetermined properties. In this connection, low-temperature methods (e.g. wet-chemical synthesis, etc.) seem to be promising.

3. Consolidation

All consolidation methods which can be cited as typical representatives for powder technology may be used in UFP processing. However, compaction, hot pressing, sintering, etc., as applied to UFPs, share some features which are connected with their activity and with the high levels of interparticle friction [92].

3.1. Compaction, and hot-pressing

Fig. 5 shows the dependence of green density on compaction pressure of Si_3N_4 compacts [101, 102]. These experiments were carried out in both conventional dies and using high-pressure devices, and cold isostatic pressing (CIP). It is obvious that the compressibility of powders decreases to a marked extent with decreasing powder size. The difference in compressibilities of different powders does not change, even at very high pressure (up to 9 GPa). Attempts to obtain compact samples of Si_3N_4 were unsuccessful, especially in the case of UFPs. The same situation occurs for TiN (Fig. 6) [103] and other UFPs (BN [104], SiC [41, 105]). It is interesting that in the case of TiN UFPs, the compressibility increases with increase in apparent density (for UFPI and UFPII, 0.27 and 0.37 $g\,cm^{-3}$, respectively) and results for magneto-impulsive and high-pressure compactions at $P \sim 3$ GPa are very similar, but at $P \sim 1$ GPa, impulsive pressure is worse.

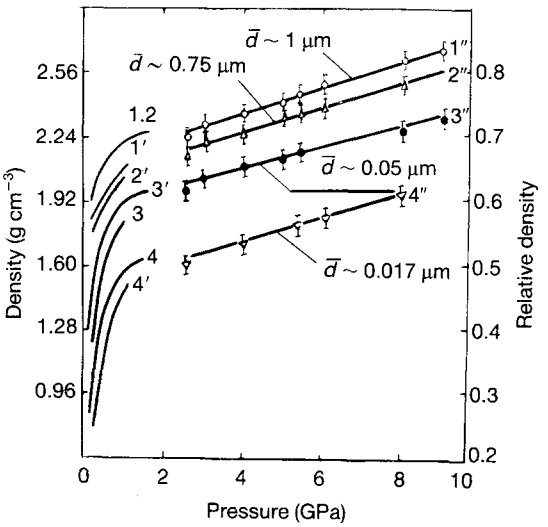

Figure 5 The effect of compaction pressure on the density of different Si_3N_4 powders (d = 0.017–1 μm). (1–4) CIP, (1′–4′) common die, (1″–4″) high-pressure device.

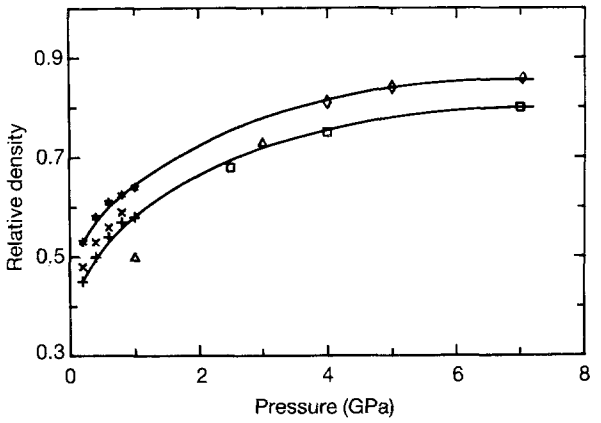

Figure 6 The dependence of relative density on compacting pressure for TiN I (+, ×, □, △) and TiN II (∗, ◇) at conventional compaction (CC), at high pressure compaction (HP), and at magneto-impulsive compaction (MI). (∗, +) 10 mm × 5 mm, CC. (×) 15 mm × 15 mm × 15 mm, CC. (◇, □) 8 mm × 5 mm, HP. (△) 7 mm × 15 mm, MI.

The poor compressibility of HMC UFPs is connected with both poor plasticity of HMC and significant interparticle friction, as mentioned above. The use of powder granulation and CIP are effective in increasing the density of green powder compacts, in absolute magnitude up to 10%. However, as indicated above, even vacuum compaction of thin compacts (~ 1 mm thick) at high pressures does not result in compact samples from metal and non-metal UFPs [1, 77]).

The results of compact investigations are of interest. Some characteristics of nc TiO_2 samples are listed in Table VII [106]. It is evident that the relative density of compacted UFPs depends strongly on the compaction temperature, but the grain size does not. It is possible that the observed results may be connected with particle grinding, as pointed out in the case of BN and TiN UFP compaction [82, 104]. It is also interesting to note that Samples A and B are assumed to have only open porosity, which is why results derived from BET and gravimetry measurements coincide very closely. Sample D is known, from BET measurements, to have only closed porosity. Accordingly, Sample C is characterized by both open and closed porosity. These results are expected to be very helpful in analysis of porosity behaviour during sintering and hot pressing.

Thus, UFP compaction at room temperature is unlikely to produce dense samples, and hot-pressing of UFPs, is therefore more preferable (see Table VII). For TiN UFPs ($S = 18\ m^2\,g^{-1}$), a relative density of about 0.98–0.99 was reached on hot pressing ($T = 1400\,°C$, $P \sim 0.5$ GPa) [107]. For comparison, the same densification during hot-pressing of TiN coarse powders has been observed only at ~ 2100 °C [108]. However, the hot-pressing conditions [107] did not conserve the nc structure; the grain size was several micrometres or more. The application of high pressures can decrease the hot-pressing temperatures and in doing so prevent, to some extent, recrystallization. Fig. 7 shows the temperature dependence of different Si_3N_4 UFP densification at P = 1.5–8.5 GPa [109–111]. It is obvious from these results that increasing the compacting pressure results in a signific-

TABLE VII Preparation conditions and properties of nc TiO_2 samples (compaction pressure ~ 1 GPa) [106]

Specimen	Temp. (°C)	Time (h)	Relative density	Grain size (nm)	Thickness (mm)	BET density
A	RT	1.25	0.62	14.8	0.561	0.62
B	290	18	0.75	11.5	0.268	0.75
C	413	5.5	0.80	10.5	0.218	0.76
D	550	7	0.92	12.5	0.240	Dense

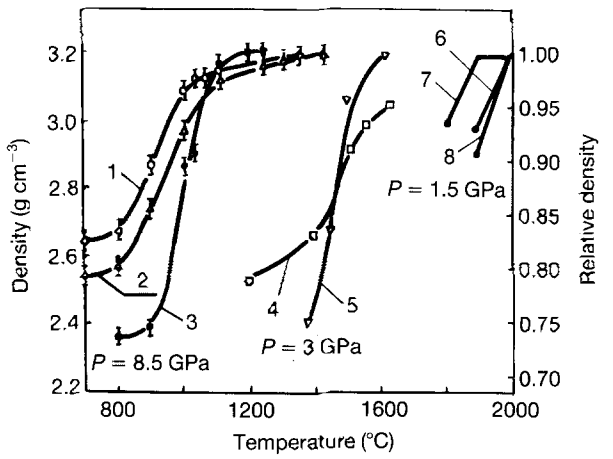

Figure 7 The dependence of temperature densification of Si_3N_4 powders on different S values at high pressures (Curves 1–3 [109]; 4, 5 [110]; 6–8 [111]). S ($m^2 g^{-1}$): 1, 1.7; 2, 2.5; 3, 37.5; 4, 4.2; 5, 23.7; 6, 23; 7, 18; 8, 13.

ant decrease of the densification temperature (from $T \sim 1900\,°C$ at $P = 1.5$ GPa to $T \sim 1100\,°C$ at $P = 8.5$ GPa). It is also interesting that the difference between common powder and UFP densification at 1200 °C almost disappears, unlike the situation at room-temperature compaction (see Fig. 5). The grain size of Si_3N_4 UFP compacted at 1200 °C ($P = 8.5$ GPa) was 0.5–1 μm (the initial particle size was ~ 0.05 μm).

Andrievski *et al.* have shown [112] that Si_3N_4 UFP densification at high pressures and high temperatures can be described approximately by HIP equations [113]. The HIP diagrams for Si_3N_4 and SiC have recently been described by Sleur *et al.* [114], and experimentally, it has been demonstrated that β-SiC UFPs ($d \sim 20$ nm) can be HIPed to a relative density 0.92 at $T \sim 1700\,°C$ ($P = 390$ MPa, $t = 3$ h) [115]. SEM and XRD investigations have revealed grain sizes of about 100 nm. For another β-SiC UFP ($d = 5$–20 nm), hot-pressing at this temperature and $P = 40$ MPa resulted in a relative density of only ~ 0.6 [41]. Increasing the temperature to 2300 °C did not give full densification (the relative density was about 0.85 and the grain size was about 1 μm).

Rapid hot-pressing of UFPs ($d = 40$–60 nm) of partially stabilized zirconia with 3 mol% Y_2O_3 (Y3–PSZ) has been investigated at 1100–1300 °C ($P = 1.6$ GPa, $t = 10$ s) [116]. Table VIII shows these results. It is evident that this processing did not result in full densification. Rapid grain growth is also a characteristic feature of these samples.

TABLE VIII Relative density (RD) and grain sizes (GS) of processed samples of Y3-PSZ UFPs [116]

Temperature (°C)	Pressure (GPa)	RD	GS (nm)
1100	0	0.72	~ 120
1200	0	0.83	~ 150
1300	0	0.94	~ 170
1100	1.6	0.87	~ 130
1200	1.6	0.93	~ 170
1300	1.6	0.97	~ 250

To our knowledge, only in the case of TiO_2 is there information available on obtaining dense samples (RD > 0.99) with a grain size of about 40 nm (initial grain size was 14 nm) [117]. These samples, with an outer diameter of ~ 3.2 mm and a length up to 5 mm, were obtained by hot-pressing at 480 °C ($P = 0.7$ GPa, RD ~ 0.9) with a final densification step, which consisted of applying a unaxial compressed load of 30 MPa. In another investigation [118] the TiO_2 dense sample (RD = 0.97) with a grain size of about 60 nm, was obtained by hot-forming at 650 °C. ($P = 57$ MPa, $t = 1800$ s, and $P = 93$ MPa, $t = 1560$ s); the initial relative density of this sample (3 mm diameter, 4–5 mm high) was 0.7. This processing is termed sinter-forging [118], although the times required for deformation were not very small. Near dense nc TiAl samples (RD > 0.95, GS = 15–21 nm) were obtained by hot-pressing at 250 °C ($P = 680$ MPa) with subsequent sintering at 500 °C [119].

3.2. Sintering

While it is evident from the foregoing that sintering cannot essentially be used to prepare dense nc HMC because of significant recrystallization, a description of this process, nevertheless, seems to be very important to our discussion. It should be borne in mind that filter and catalyst preparation is obtained by UFP sintering. This scientific problem is well known, and it is no surprise that the study of UFP sintering began about 20 years ago or more (see, for example, [120, 121]). These investigations have stimulated the interest of catalysis specialists and interest in sintering theory development. German [122] has analysed the $\Delta S/S$ reduction kinetics for UFP sintering using Frenkel–Kuczynski's approach. Surface diffusion-controlled sintering has been observed in the initial stage of sintering of many submicrometre sized oxide powders (Al_2O_3, TiO_2, etc.). The change of S for nitride UFPs on sintering has been analysed by Troitskiy *et al.* [123].

It is common knowledge that the sintering temperature of UFPs is substantially below that for common powders. This difference, which is due to more significant values of capillary forces and more favourable particle structure, may be up to several hundred degrees. As stated above, this difference also occurs during hot-pressing, and this is one of the advantages of UFP applications.

The results of investigations of some UFP densification during sintering are shown in Figs 8–11 [27, 124, 125]. Typical densification S-curves are characteristic features of TiN, TiO_2 and ZrO_2 UFP densification, as observed in Figs 8–10. Some additional information on sintering of ZrO_2 UFPs, is shown in Table IX [126]. The significant rate of recrystallization and densification seen in these results is characteristic of ZrO_2 UFPs. This has also been reported by other investigators [116, 125]. However, Si_3N_4 powders, even UFPs, are very difficult to densify without sintering aids (Fig. 11) [124], which is connected with the covalent origin of Si_3N_4 and its poor diffusional

and dislocation mobilities. For covalent solids (boron, silicon, Si_3N_4, SiC, etc.) the estimated active densification temperature during sintering is about 0.85 T_m or higher, as is shown in Fig. 12 [127].

TABLE IX Influence of sintering conditions on grain size and density of ZrO_2 UFPs [126]

Sintering conditions	Grain size (nm)	Density ($g\,cm^{-3}$)
RT	5	2.442
700 °C/15 h	25	3.197
700 °C/15 h + 900 °C/21 h	80	4.184
700 °C/15 h + 900 °C/21 h + 1100 °C/18 h	155	5.340 (RD = 0.93)

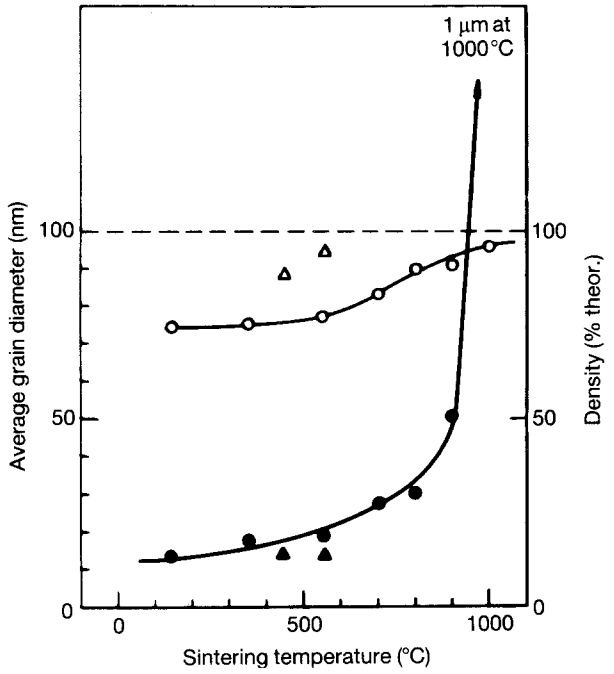

Figure 8 Density (○, △) and grain size (●, ▲) of TiO_2UFP as a function of sintering and hot-pressing temperature (t = 15–20 h) [125]. P (GPa): (○, ●) ○, (△, ▲) 1.

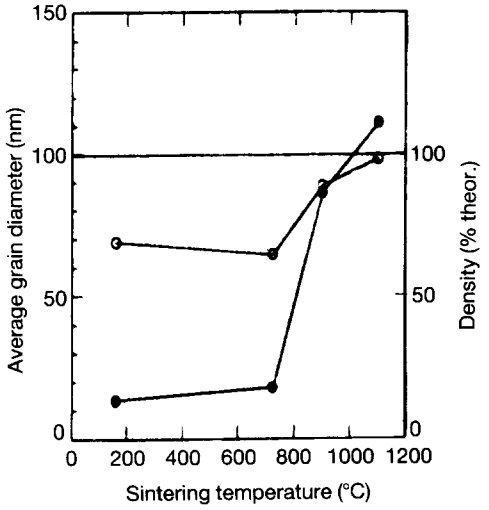

Figure 9 As Fig. 8, for ZrO_2 UFP [125]. (○) Density, (●) grain size.

This graphical display of the densification data [92] is supplemented by TiO_2, TiN, ZrO_2, and Al_2O_3 UFP results [27, 125, 128]. Thus, for metal-similar HMCs (TiN type) and ionic oxides (ZrO_2 type), the applica-

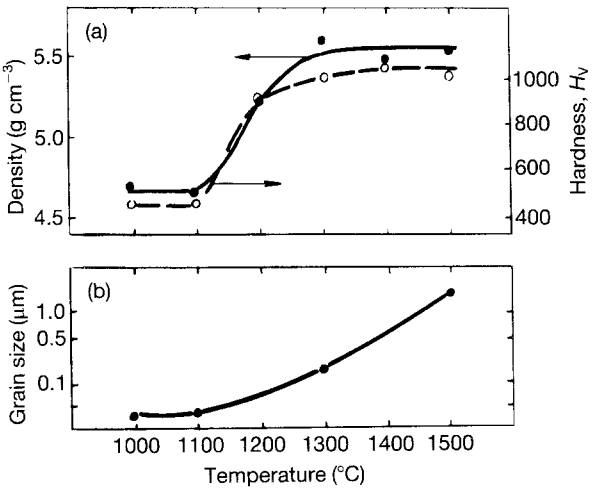

Figure 10 (a) (●) Density, (○) hardness, and (b) grain size versus sintering temperature for TiN UFP (t = 5 h) [27].

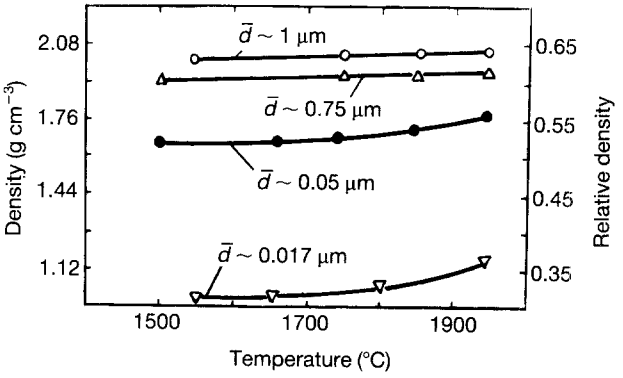

Figure 11 Density as a function of sintering temperature for different Si_3N_4 powders (P_{N_2} = 30 MPa, t = 5 h).

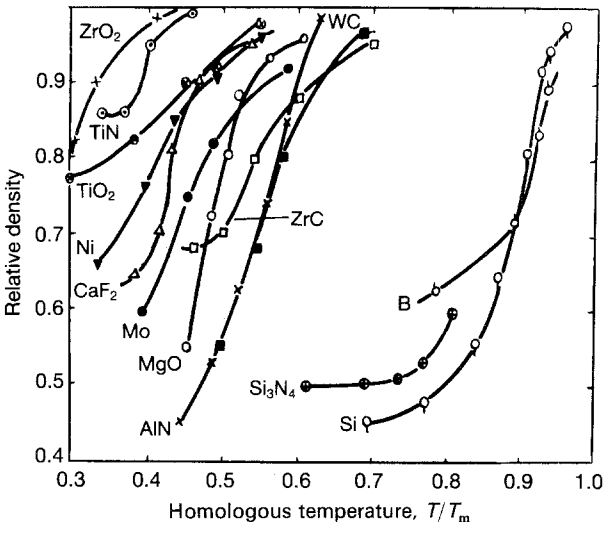

Figure 12 Densification of different powders, including UFP (TiN, ZrO_2, TiO_2, Ni, AlN, Si_3N_4, etc.), as a function of homologous temperature.

tion of UFPs is accompanied by decreasing sintering temperatures, and in the case of covalent solids (Si_3N_4 and most probably BN, B_4C, SiC, etc.) the UFPs application does not seem so effective.

An interesting possibility of rapid liquid-state sintering to obtain nc hard alloys has been described [53]. A dense structure in WC–10 wt % Co derived from UFP can be achieved in 30 s at 1400 °C, which gives a WC grain size of about 200 nm. It should be noted that an additional 30 s sintering time leads to a ten-fold increase in grain size (up to 2 μm).

Ragulia [129] called attention to the possibility of rate-controlled sintering (RCS). Dense nc nickel (RD = 0.98, GS = 70–80 nm) was obtained using RCS; RCS is likely to be used to obtain nc HMC.

One interesting example of superactivated sintering of nc TiO_2 has been demonstrated by Kumar *et al.* [130]. Dense nc titania (RD > 0.99, average grain size < 60 nm) can be prepared by sintering titanium oxide sol–gel (primary particle size ~ 6 nm) near the anatase–rutile phase transformation temperature (about 600 °C). The increased diffusional mobility during phase transformation is suggested to enhance the sintering rates at lower temperatures.

As far as we know, the application of this method of preparing nc materials by crystallization from amorphous state has never been investigated for nc HMC.

3.3. High-energy methods

Other possible methods of powder compaction can also be applied to UFP consolidation. From the above it is clear that high-energy methods are of interest. However, information on this is not great and is essentially exhausted by some observations on shock compaction, hot-forging, and electro-discharge compaction. Generally, UFP consolidation methods are similar to those for amorphous materials [73, 131]. The problems of retaining the amorphous state or nc structure are in many ways similar during consolidation.

Kondo and co-workers [132–134] studied the shock-compression features of some ceramic powders (SiC, Al_2O_3, MgO, Si_3N_4, BN, diamond, etc.). Under the shock-compaction conditions, the powder particle surface can melt, fuse, and solidify. Shock duration is supposed to be ≤ 1 μs and hence the powders can be consolidated without significant grain growth. Thus good nc SiC compacts with RD = 0.97 were obtained under optimum impact conditions (velocity = 2.5 km s^{-1} for initial RD 0.7) [132]. This result is related to the powder having an average particle size of 280 nm. XRD line-broadening analysis has indicated a microstrain increase and a grain size decrease. Some problems still remain in applying the shock-compaction method, namely macrocracks and the general yield.

Kovtun *et al.* [135, 136] have described successful experiments on sintering sphalerite and wurtzite modifications of BN in shock waves. Nanocrystalline structure, high values of relative density and hardness (porosity 3–5%, H_V = 43–80 GPa) in polycrystals of 16–18 nm diameter and 4 mm long, have been obtained in many experiments.

MgO UFP (d ~ 10 nm) was hot-forged at 15 GPa in a molybdenum die at 1300 °C after preheating for 10 min [137]. The maximum relative density value (~ 0.99) was obtained at 30% deformation ratio. In doing this, the grain size was 100–150 nm. This value is a result not only of recrystallization but also the mechanical fracture which took place.

A high-voltage high-density electric current pulse was applied whilst compacting TiN UFPs (S ~ 90 $m^2 g^{-1}$) [138]. However, only samples with a relative density about 0.87 were obtained. Such processing was also used for obtaining $NbAl_3$ samples from mechanical alloyed UFPs [148]. XRD analysis has revealed grain sizes in the range 22–100 nm. Information on relative density values is absent.

4. Properties

4.1. Structure and recrystallization

The main feature of nc materials is the large fraction of their atoms that are accommodated in grain boundaries, which results from their nc structure. It is easy to estimate the fraction of atoms associated with grain boundaries as a function of grain size, as shown in Fig. 13 [3]. These estimations were fulfilled for two possible values of grain boundary thickness: 0.5 and 1.0 nm. It is evident that for a 100 nm grain size, this fracture falls to about 1%–3%. In this connection it is clearly of interest to study this aspect. Some results have been obtained by Gleiter, Siegel and their coworkers using samples prepared by the gas-condensation method [1–3, 14]. The structure was investigated by TEM, including high-resolution electron microscopy, SEM, XRD, small-angle neutron scattering (SANS), and Mössbauer, Raman, and positron annihilation spectroscopy (PAS).

For nc TiO_2 [3, 139] the following conclusions have been drawn:

1. Evidence derived from Raman scattering results,

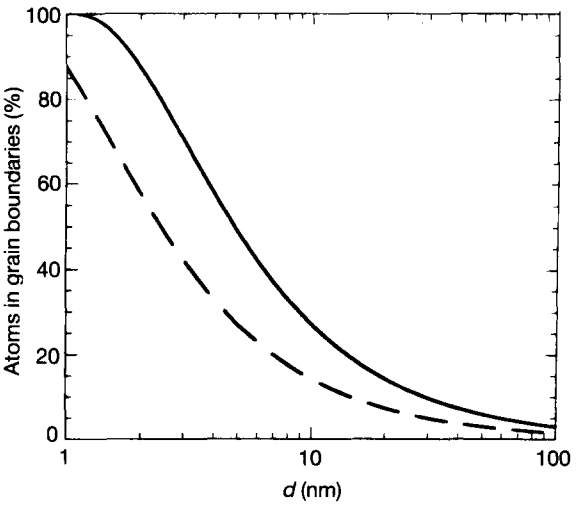

Figure 13 Percentage of atoms in the grain boundaries of an nc material as a function of grain diameter, assuming the average grain boundary thickness ranges from 0.5–1.0 nm (~ 2–4 atomic planes wide) [3]. (— — —) 0.5 nm, (———) 1.0 nm.

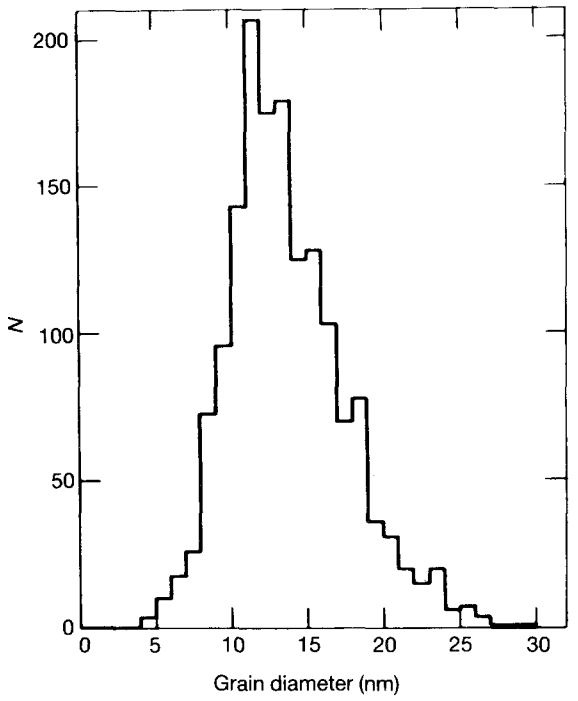

Figure 14 Grain-size distribution for an nc TiO_2 (rutile) sample compacted to 1.4 GPa at room temperature, as determined by TEM [3].

indicates there are no "gas-like" random structural components at the grain boundaries.

2. The grain size distribution for the as-compacted sample is rather narrow and similar to the typical log-normal particle size produced by the gas-condensation method (Fig. 14).

3. SANS and PAS results have revealed the availability and educational development of microvoids during sintering.

As a whole, recent investigations of nc materials indicate that the structure of their grain boundaries is quite similar to that in coarser-grained, conventional materials [139].

The nc HMC grain boundary properties are in the process of investigation. The evolution of nc particle contact interfaces to grain boundaries, as applied to plastic objects, has been analysed by Gryaznov *et al.* [140]. Morochov *et al.* [75] drew attention to the possibility of lower free energy of nc particles with the formation of phase inhomogeneity in the bulk and on the surface. The surface layers may be enriched with high-temperature modifications that have a higher symmetry and lower density. Some information on internal friction of nc ZrO_2 ($T = -200$ to $+20\,^{\circ}C$) has been reported by Xie *et al.* [126]. Thermodynamic measurements of grain-boundary energy have revealed for SiC and TiO_2 a value of 1–3 $J\,m^{-2}$[141]. However, from the results on TiO_2 UFP sintering [130], it follows that the surface energy value was 1.1 $J\,m^{-2}$. The primary data on grain-boundary self-diffusion in nc TiO_2 have been obtained by Hofler *et al.* [142].

Figs 8–10 and Table VIII have shown the grain size growth during sintering for TiO_2, ZrO_2, and TiN UFPs [27, 125]. It is obvious that substantial grain growth takes place after the relative density exceeds ~ 0.9. At 6%–8% porosity, all pores become closed (see earlier Table VII). These are almost common rules for all porous materials [92]. However, the optimum pore size is supposed to need refinement for effective prevention of recrystallization. Yttrium impurities in nc TiO_2 have been shown [125] to be effective in stopping grain growth. Results for the isothermal annealing of nc TiO_2 without additions (RD ~ 0.9) were shown to fit a growth law of the form

$$L^3 - L_0^3 = \alpha t^n \exp(-Q/RT) \qquad (2)$$

where L is GS, $L_0 = 14$ nm, $n = 1.1$–1.15, $\alpha = 7.29 \times 10^{17}\,nm^3\,s^{-1}$, $Q = 278\,kJ\,mol^{-1}$. The power 3 in Equation 2 is typical for porous body recrystallization.

The peculiarities of nc BN recrystallization and plastic deformation during high-pressure and high-temperature treatment have been analysed in detail by Pilyankevich and Oleinik [143]. It should be noted that dynamic recrystallisation may be of interest as a method for nc material preparation.

4.2. Mechanical properties

Hardness is one of the most extensively studied properties of nc HMC. Table X gives the results. It should be noted that results for shock-compaction samples are characterized by a high level of scattering [132–134, 136] (in Table X only the best results are cited). However, even against this background, the results for samples derived from other methods seem very poor. For SiC, TiO_2, ZrO_2, TiN, MgO and Al_2O_3, the hardness values in Table X are at best quite similar to those for coarser-grained, conventional materials based on HMCs or their single crystals [6]. It is worth pointing out that in the case of nc metals (copper, palladium, nickel, silver) the hardness in-

TABLE X Hardness of some nc HMC

HMC	RD	GS (nm)	H_V (GPa)	Preparation method
SiC [132]	0.97	60–100	26.4	Shock-compaction
WC–Co [53]	~ 1.0	200	19.5	Short liquid-state sintering and HIP
TiO_2 [125]	0.94	14	10.5	Compaction after gas-condensation method
ZrO_2 [116]	0.97	250	14	Rapid hot-pressing
MgO [137]	0.99	100–150	8–10	Hot forging
Al_2O_3 [133]	0.94	70	14	Shock compaction
TiN [27]	~ 0.99	200	10	Sintering
BN [136]	0.96	25	43–80	Shock compaction
C [134]	0.91		63–68	Shock compaction
	0.94		56–65	

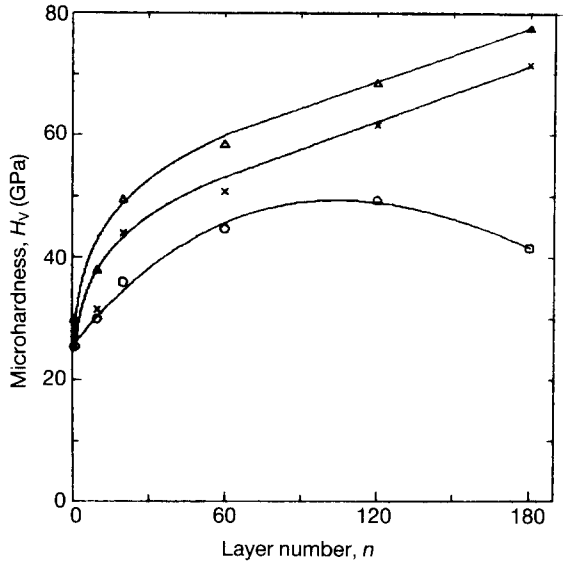

Figure 15 Influence of the number of layers on nitride film hardness. (△) TiN–NbN, (×) TiN–ZrN, (○) TiN–CrN.

crease on average, four to six times, as a result of grain size decrease [144–146]. Finally, a study of HMC film hardness results also evinces the possibility of increasing the nc HMC hardness [8, 145]. Fig. 15 shows the influence of the number of layers on the hardness of TiN–ZrN, TiN–NbN, and TiN–CrN PVD films which had similar total thicknesses (near 2 μm) [147]: the significant H_V increase is evident. There are at least three physical reasons for such an increase: interface boundaries stop crack propagation, the grain size has a low value in monolayers (equal to, near to or smaller than the layer thickness), and possibly a more favourable situation exists with residual strains in multilayer films. The porosity and internal stresses influence the not so small values of grain size and possibly other factors may be the reasons for the not so high hardness values of some nc HMC in Table X.

Fig. 16 shows the hardness of two samples of nc TiO_2 with different relative density values as a function of grain size [125]. The Hall–Petch-like behaviour and the influence of porosity level are evident. The dependence of hardness on WC grain size in WC–10 wt % Co hard alloys which were prepared from chemically processed powders with Sanvik's fine and nanofine grades, is shown in Fig. 17 [53].

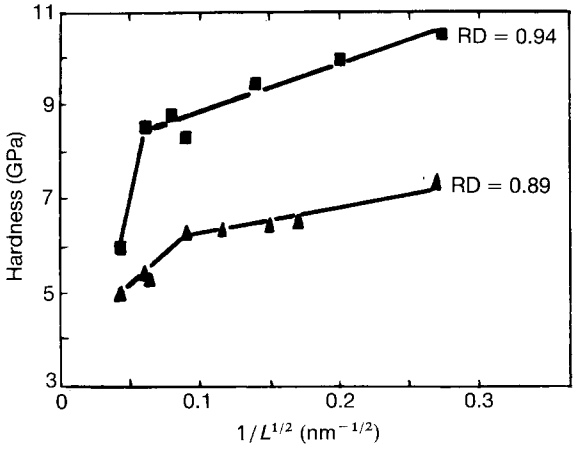

Figure 16 Hardness of nc TiO_2 as function of grain size [125].

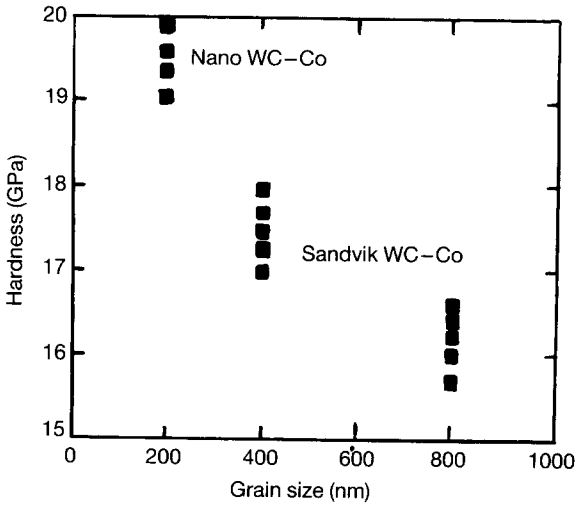

Figure 17 Dependence of hardness on WC grain size in WC–10 vol % Co hard alloys [53].

The nature of the influence of grain size on the hardness of nc materials is the subject of wide speculation. It is known that both a Hall–Petch-like and an inverse Hall–Petch-like behaviour exist as does a mixture of the two (see, for instance, [119, 144–146, 148]). The conventional relationship of the influence of grain size on metal and alloy hardness is described by the well-known Hall–Petch equation

$$H = H_0 + kL^{-1/2} \quad (3)$$

where H_0 and k are constants. An example of the inverse Hall–Petch-like behaviour for nc TiAl is shown in Fig. 18 [119]. A non-monotonic dependence has been pointed out for nc $NbAl_3$ [148]. In this case, the maximum hardness value was observed for samples with $L \sim 60$ nm. This value for nanocrystalline copper and palladium has been observed at an interval lower than 10 nm. [149]. From common knowledge it is clear that with decreasing grain size the role of grain-boundary sliding can be increased. Thus the availability of the non-monotonic dependence $H = f(L)$ seems very likely. The role of dislocations and admixtures is also very important. It is interesting that intergranular fracture is typical for nc TiO_2 sintered at

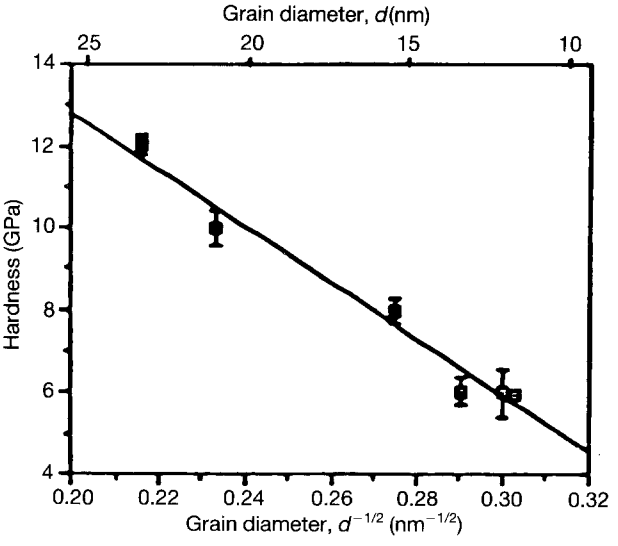

Figure 18 Grain-size effect on the hardness of nc TiAl [119].

temperatures below 1000° C and only at about 1100° C is completely transgranular fracture observed [150]. However, in summary, the real physical reasons for the behaviour of both plastic nanocrystalline metals, nanocrystalline brittle intermetallics, and nanocrystalline HMC, i.e. changing hardness with grain size, are, at present, unclear.

Another very important mechanical feature of nc HMC is creep, including superplasticity. This property is the distinctive antipody of hardness. Karch *et al.* [151] reported that porous nc TiO_2 is allowed to deform plastically during indentation testing at low temperature. A detailed investigation of low-temperature creep of nc TiO_2 (RD = 0.99, L = 40 nm) has been carried out by Hahn and Averback [117]. At 600–800° C for compression stresses up to 50 MPa, the authors concluded that diffusional creep is the dominant mode of deformation in nc TiO_2 because of the low dislocation density. However, unlike both Nabarro–Herring and Coble creep which depend linearly on stress, i.e. the stress exponent of the strain rate $n = 1$, their results indicate that $n = 3$. The grain-size dependence was also found to be unusual, $L^{1-1.5}$. It was supposed that the creep mechanism was interface-reaction controlled, so the relation for creep rate, $\dot{\varepsilon}$, takes the form

$$\dot{\varepsilon} = A\sigma^3 L^{-(1-1.5)} \exp(-Q/RT) \quad (4)$$

where A is a constant and Q is the activation energy.

Grain-boundary sliding is suggested as the principal mechanism for sinter-forging of nc TiO_2 [118].

It is common knowledge that brittle HMC, especially such covalent solids as Si_3N_4, SiC, etc., are difficult to deform. It is very attractive to induce their deformation under nanocrystalline conditions. Wakai *et al.* [152] revealed the superplasticity in the Si_3N_4–SiC system with oxide additions for liquid-phase formation. In these samples the grain size was 200–500 nm and uniform superplastic deformation at 1600° C was > 150% (σ = 50 MPa). In our experiments, superplasticity was observed in the systems of Si_3N_4–TiB_2 (Fig. 19) [145, 153]. For compositions with 25 vol % S_3N_4, the maximum creep rate (the whole deformation was about 30%) was fixed. This anomaly was displayed only when the Si_3N_4 UFPs were used and their grain size in hot-pressed samples was near 500 nm (the TiB_2 grain size was about 2 μm). Superplastic deformation of nanocrystalline SIAlONs at 1550–1600° C has been reported [154]. The grain size in these experiments was about 100–200 nm.

The reported results [117, 118, 152–154] seem to be only the first step in the exploration of the very important problem of HMC superplastic forming. The main difficulties of obtaining nc structure and its conservation during processing still remain to be resolved.

Information on other nc HMC mechanical properties is very poor and sparse. Some data on the elastic properties of porous nc TiO_2 and nc ZrO_2 have been reported [126, 155]. The fracture toughness, K_{IC}, value of nc MgO (see Table X) was about 1–1.5 MPa $m^{1/2}$ [137]. Kodama and Miyoshi reported the non-monotonic grain-size dependence of K_{IC} in an

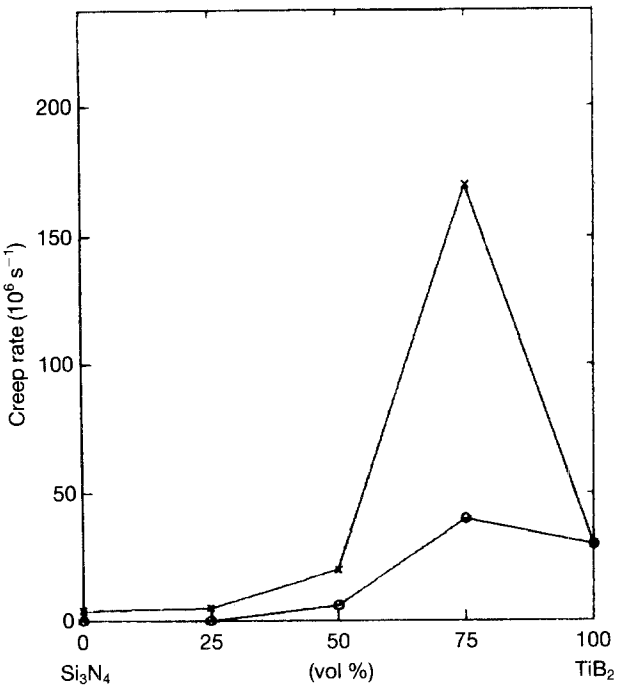

Figure 19 Creep rate change in the system Si_3N_4–TiB_2 (T = 1600 °C, t = 30 min, σ = 20 MPa). L (μm): Si_3N_4 (×), 0.5; Si_3N_4 (○), 2–4; TiB_2, 2.

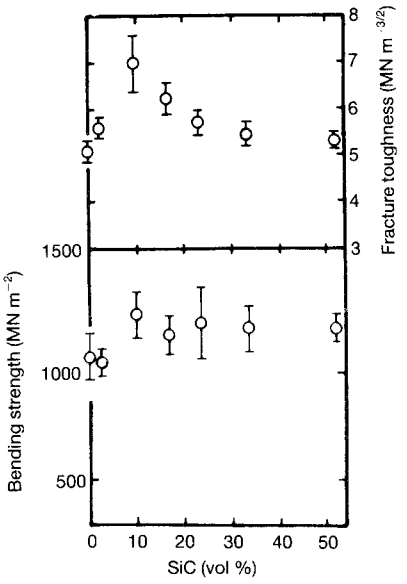

Figure 20 Fracture toughness and bending strength of Si_3N_4/SiC nanocomposite as a function of nc SiC vol % [159].

SiC sample of 0.2–1.4 μm [156]. K_{IC} showed a maximum ($\sim$ 5.1 MPa $m^{1/2}$) at the average grain size $\sim$ 0.7 μm (for all samples the relative density was about 1.0). Hardness measurements of porous and polycrystalline nc TiO_2 in the temperature range 25–1200° C indicated that nc TiO_2 was more ductile [157]. However, K_{IC} measurement has not revealed any influence of grain size (L = 14–500 nm, RD $\sim$ 0.9) for this compound ($K_{IC} \sim$ 1.5 MPa $m^{1/2}$) [158].

Niihara *et al.* [159, 160] reported some properties of hot-pressed nanocomposite materials composed of an Si_3N_4 matrix and nanometer-sized SiC particles. The effect of SiC volume content on bending strength and K_{IC} is shown in Fig. 20. It is evident that mechan-

ical properties are improved by introducing ~ 10 vol % SiC. This nanocomposite including 32 vol % SiC was characterized by improved strength above 1200° C [160].

4.3. Physical and other properties

These investigations are in the earliest stage. Some electrical and thermo-physical properties of Ni–ZrO_2, TiN–AlN and Si_3N_4–SiC nanocomposites have been investigated [161–164]. The critical point in the Ni–ZrO_2 system is 25–30 vol % Ni [161, 162], and that in the Si_3N_4–SiC system is about 17 vol % SiC [159]. The latter value agrees with the percolation theory. The existence of special interphase grain boundaries with a minimal phonon scattering has been revealed in the TiN–AlN system [164].

The increase of critical magnetic field, H_{c_2}, with decreasing particle size of nitrides (NbN, VN, TiN, NbNC) has been observed by Domashnev [165] and Troitskiy *et al.* [166]. The decrease of particle size from ~ 75 nm to ~ 15 nm results in an H_{c_2} increase of about twice.

We conclude by examining one important physico-chemical aspect of the development of nc materials. This is the influence of particle size on phase equilibria. The problem was examined by Morochov *et al.* [75] with the Al–Si and ZrC–C systems as examples. It is shown that the decline in the eutectic temperature, ΔT_e, resulting from the influence of the particle size of one component is estimable in the regular-solution approximation from the following relations [167]

$$\Delta T_e = \Delta F_2^s / R \ln x_s \quad (5)$$

$$\Delta T_e = \Delta F_2^s / R \ln x_e - \Delta s_2 \quad (6)$$

$$\Delta T_e = \Delta F_1^s / R \ln(1 - x_e) \times (1 - x_s)^{-1} - \Delta s_1 \quad (7)$$

where ΔF_i^s is the contribution made by the excess surface energy, which is written in per mole terms as $\Delta F_i^s = 3V_i\sigma_i/r_i$ (V_i is the molar volume, σ_i is the specific surface energy, and r_i is the particle radius), x_s and x_e are the concentrations corresponding to maximum solubility and eutectic, ΔS_i is the entropy of fusion, and R is the gas constant.

The eutectic TiC–TiB_2 and TiN–TiB_2 systems were utilized to consider the influence of particle size on ΔT_e, as shown in Table XI [167]. Estimates of ΔT_e from Equations 5–7 were virtually identical and indicated that a significant decline of T_e should be expected for $r < 10$–20 nm. Such estimations for the nanocrystalline TiN–AlN system were made by Andrievski and Anisimova [168].

Although these results can present only an approximate estimate, the possibility of decreasing T_m in nanocrystalline materials must be taken into account in further research and development of these materials, as applied especially to two-phase systems. It is also evident that experimental study of phase equilibrium in nanocrystalline systems is necessary.

TABLE XI The influence of the particle size of one component in the TiC (TiN)–TiB_2 systems on change in eutectic temperature (T_e = 2790 K, $TiC_{0.95}$–TiB_2; T_e = 2870 K, $TiN_{0.93}$–TiB_2 [6])

Particle radius	$-\Delta T_e$ (K)	
(nm)	TiC(TiN)–TiB_2	TiB_2–TiC(TiN)
100	~ 45	~ 35
50	~ 90	~ 70
10	~ 450	~ 350
5	~ 900	~ 700

5. Applications and conclusion

It is seen that information on consolidation and properties of nc HMC is not very comprehensive nor exhaustive. The data on UFPs are more impressive. Therefore, possible applications can only be put forward in very common terms. Catalysis, filters, tool materials and ductile ceramics are the main fields of nc HMC application. It is possible to add UFP application as additions to conventional materials. Perhaps detailed investigations of nc HMC electrical and magnetic properties will reveal possible new applications. As applied to our review, of special interest is the application of nc HCP as tool and structured materials. In this connection, the results (see Fig. 17) [53] show considerable promise. A high value of K_{IC} (15–18 MPa $m^{1/2}$) has been reported for nc superhard materials based on wurtzite-like BN (materials of the Hexanite type) [169, 170]. Feldmuehle Inc. (The Netherlands) has also developed a superhard material based on wurtzite-like BN produced by explosive synthesis, with a grain size of 20 nm (K_{IC} = 13–22 MPa $m^{1/2}$) [171].

Ductile nc intermetallic compounds and ceramics are considered to be quite feasible [2, 172]. Nanophase Technologies Corporation (USA) and Katerpillar Inc. (USA) are reported to receive a US 1 million $ award by the Federal Advanced Technology Program to support production and use of nc ceramic powders (particle size of the order of 10 nm) for diesel engines [173].

It is clear, therefore, that many nc HMC could be candidates for new superhard material development, on the one hand, and new ductile materials, on the other. However, the realization of this statement is in its infancy.

It is possible to agree with Gleiter's statements that economical methods to produce a sufficient quantity of nc materials and the thermal stability of their structure are the basic problems [2]. To sum up, further research into powder preparation and consolidation is required. In addition, detailed investigation of structure, and physical, chemical, and mechanical properties, including the developmental theory of nc HMC, will help to eliminate the lack of sufficient data and of an understanding of the nature of these phases, thus resulting in an enlargement of their industrial applications.

Acknowledgements

The author thanks Professor V. N. Troitskiy and Professor L. I. Trusov for useful discussions, and Dr I. I. Korobov, Dr V. I. Torbov, Dr S. V. Gurov and

Mrs Olga A. Datchenko for their help in manuscript preparation.

References

1. H. GLEITER, *Progr. Mater. Sci.* **33** (1989) 223.
2. H. GLEITER, *Nanostruct. Mater.* **1** (1992) 1.
3. R. W. SIEGEL, *Ann. Rev. Mater. Sci.* **21** (1991) 559.
4. C. SURYANARAYANA and F. H. FROES, *Metall. Trans.* **23A** (1992) 1071.
5. R. A. ANDRIEVSKI, *Sci. Sinter.* **20** (1988) (Special Issue 1) 49.
6. R. A. ANDRIEVSKI and I. I. SPIVAK, "Strength of High-Melting Compounds and Materials on Their Base" (Metallurgy, Chelyabinsk, 1989) (in Russian).
7. M. G. HOCKING, V. VASANTASREE and P. S. SIDKY, "Metallic and Ceramic Coatings: Production, High-Temperature Properties and Applications" (Harlow, London, 1989).
8. D. S. RICKERBY and A. MATTHEWS, *Rev. Powd. Metall. Phys. Ceram.* **4** (1991) 15.
9. R. W. CHORLEY and P. W. LEDNOR, *Adv. Mater.* **4** (1991) 474.
10. M. KATO, *Jpn. J. Appl. Phys.* **14** (1975) 181.
11. *Idem. ibid.* **15** (1976) 757.
12. R. UYEDA, *Progr. Mater. Sci.* **35** (1991)1.
13. B. GUNTHER and A. KUMPMANN, *Nanostruct. Mater.* **1** (1992) 27.
14. H. HAHN and R. S. AVERBACK, *J. Appl. Phys.* **67** (1990) 1113.
15. S. IWAMA, K. HAYAKAMA and T. ARIZUMI, *J. Cryst. Growth* **56** (1982) 265.
16. *Idem. ibid.* **66** (1984) 189.
17. G. SKANDAN, H. HAHN and J. C. PARKER, *Scripta. Metall. Mater.* **25** (1991) 2389.
18. A. E. KRAVCHIK and V. S. NESHPOR, *Powd. Metall.* (4) (1976) 14 (in Russian).
19. L. T. GANKEVICH, S. G. TITOV, S. L. BOCHKOV, T. Kh. UZBEKOVA, E. M. CHEREDNIK and A. F. KUTEINIKOV, *ibid.* (9) (1987) 1.
20. W. G. SCHMIDT, *Interceram.* **40** (1991) 15.
21. S. E. WITTER, in Report of the Investigation Bureau Mines, US Department of the Interior (1984) N8854, p. 12.
22. V. Ju. DAVIDKIN, L. I. TRUSOV, P. Ju. BUTIAGIN, I. V. KOLBANEV, V. F. PETRUNIN, V. I. NOVIKOV and A. V. BURCHANOV, in "Physics-Chemistry of Ultradispersed Systems", edited by Ja. K. Vaivads (Latvian AS, Riga, 1989) p. 187 (In Russian).
23. G. Lé GAER, E. BAUER-GROSSE, A. PIANELLI and E. BOUZY. *J. Mater. Sci.* **25** (1990) 4726.
24. P. MATEAZZI and G. Le. GAER, *J. Am. Ceram. Soc.* **74** (1991) 1382.
25. A. CALKA and A. RADINSKI, *J. Less-Common. Metals* **161** (1990) L23.
26. A. CALKA and J. WILLIAMS, *Mater. Sci. Forum* **88–90** (1992) 787.
27. Y. OGINO, M. MIKI, T. YAMASAKI and T. INUMA, *ibid.* **88–90** (1992) 795.
28. A. V. KURDIUMOV and A. N. PILIANKEVICH, "Phase Transitions in Carbon and Boron Nitride" (Naukova Dumka, Kiev, 1979) (in Russian).
29. I. N. Frantsevitch (ed.) "Superhard Materials", (Naukova Dumka, Kiev, 1980) (in Russian).
30. B. BERGMAN and J. BARRINGTON, *J. Am. Ceram. Soc.* **49** (1966) 502.
31. V. V. SCOROCHOD, G. I. SAVVAKIN, S. M. SOLONIN and L. L. KOLOMIETS, *Powd. Metall.* (8) (1974) 80 (in Russian).
32. Sh. EIDELMAN and A. ALTSHULER, in "Abstracts of First International Conference on Nanostructured Materials" (Academia Mexicana, Cancun, 1992).
33. V. N. TROITSKIY, S. V. GUROV and V. I. BERESTENKO, *Chem. High Energy* **13** (1979) 267 (in Russian).
34. V. M. BATENIN, I. I. KLIMOVSKIY, G. V. LYSOV and V. N. TROITSKIY, "RF-Plasma Generators. Physics, Engineering, Applications" (Energoatomizdat, Moscow, 1988) pp. 175–214 (in Russian).
35. T. N. MILLER, *Inorg. Mater.* **15** (1979) 557 (in Russian).
36. *Idem, ibid.* **15** (1979) 595 (in Russian)
37. T. N. Miller (ed.) "High-Temperature Synthesis and Properties of High-Melting Compounds", (Zinatne, Riga, 1979) (in Russian).
38. T. Ja. KOSOLAPOVA, G. N. MAKARENKO and D. P. ZIATKEVICH, *Mendelev Chem. J.* **24** [3] (1979) 30.
39. V. D. PARCHOMENKO, P. I. SOROKA, Yu. I. KRASOKUTSKII and V. I. VERESCHAK, *ibid.* **36** [2] (1991) 62.
40. K. ISHIZAKI, T. EGASHIRA, K. TANAKA and P. B. CELLS, *J. Mater. Sci.* **24** (1989) 3553.
41. K. KIJIMA, H. NOGUCHI and M. KONISHI, *ibid.* **24** (1989) 2929.
42. F. ALLAIRE and S. DALLAIRE, *ibid.* **26** (1991) 6736.
43. H. J. LEE, K. EGUCHI and T. YOSHIDA, *J. Am. Ceram. Soc.* **73** (1990) 3356.
44. I. V. BLINKOV, A. V. IVANOV and I. E. OREKHOV, *Phys. Chem. Proc. Mater.* (2) (1992) 73 (in Russian).
45. Ja. A. KRASTIN'SH, U. A. ZIELEN, L. M. CHERA and T. N. MILLER, *Trans. Latv. Acad. Sci. ser. Chem.* (6) (1978) 651 (in Russian).
46. G. P. VISSOKOV, K. D. MANOLOVA and L. B. BRAKALOV, *J. Mater. Sci. Lett.* **16** (1981) 1716.
47. J. D. CASEY and J. S. HAGGERTY, *J. Mater. Sci.* **22** (1987) 737.
48. R. FANTONI, E. BORSELLA, S. PICCIRILLO, R. CECCATO and S. ENZO, *J. Mater. Res.* **5** (1990) 143.
49. R. A. BAUER, J. G. M. BECHT, F. E. KRUIS, B. SCARLETT and J. SCHOONMAN, *J. Am. Ceram. Soc.* **74** (1991) 2759.
50. E. V. PRILUTSKI, L. T. DOMASEVICH, A. V. NESHPOR and T. Ja. KOSOLAPOVA, in "Carbides and Materials on Their Base", edited by T. Ja. Kosolapova (Ukranian Academy of Sciences, Kiev, 1983) p. 123 (in Russian).
51. P. T. B. SHAFFER, K. A. BLAKELY and M. A. JANNEY, *Adv. Ceram.* **21** (1987) 257.
52. T. S. BARTNITSKAJA, L. A. IVANCHENKO, T. Ja. KOSOLAPOVA, *Powd. Metall.* (6) (1988) 52 (in Russian).
53. L. E. McCANDLISH, B. H. KEAR and B. K. KIM, *Nanostruct. Mater.* **1** (1992) 119.
54. L. I. TRUSOV, Ju. A. VOSKRESENSKIY, I. A. REPIN, V. I. NOVIKOV. V. N. LAPOVOK, V. N. TROITSKIY and S. S. PLOTKIN, *Powd. Metall.* (7) (1989) 17 (in Russian).
55. N. HASHIMOTO, H. YODEN and Sh. DEKI, *J. Am. Ceram. Soc.* **75** (1992) 2098.
56. A. N. ZELIKMAN, O. B. BISTROVA and L. N. LEONOVA, in "Metallurgy of Rare Metals. Powder Metallurgy" (Metallurgia, Moscow, 1987) p. 39 (in Russian).
57. K. SU, M. NOWAKOWSKI, D. BONNELL and L. G. SNEDDON, *Chem. Mater.* **4** (1992) 1139.
58. V. I. SHAPOVAL, CH. B. KUSHKHOV and I. A. NOVOSELOVA, *J. Appl. Chem.* **58** (1985) 1027 (in Russian).
59. O. N. GRIGORIEV, CH. B. KUSHKHOV, A. M. SHATOCHIN, G. B. KHOMENKO and A. A. TISCHENKO, *Powd. Metall.* (8) (1991) (in Russian).
60. D. ZENG and M. J. HAMPDEN-SMITH, *Chem. Mater.* **4** (1992) 968.
61. R. L. AXELBAUM, S. E. BATES, W. E. BUHRO, C. FREY, K. F. KELTON, S. A. LAWTON and S. M. SASTRY, in "Abstracts of First International Conference on Nanostructured Materials" (Academia Mexicana, Cancun, 1992).
62. G. FRANZ and G. SCHWIER, in "Raw Materials for New Technologies", edited by M. Kursten (Nagele and Obermiller, Stuttgart, 1990) p. 139.
63. S. SCHWIER, G. NIETFELD and G. FRANZ, *Mater. Sci. Forum* **47** (1989) 1.
64. H. KODAMA and T. MIYOSHI, *Adv. Ceram. Mater.* **3** (1988) 177.
65. Th. HOURS, P. BERGEZ, J. CHARPIN, A. LARBOT, Ch. GUIZARD and L. COT, *Am. Ceram. Soc. Bull.* **71** (1992) 200.

66. M. ADACHI, K. OKUYAMA, S. MOON, N. TOHGE and Y. KOUSAKA, *J. Mater. Sci.* **24** (1989) 2275.
67. R. RIEDEL, K. STRECKER and G. PETZOW, *J. Am. Ceram. Soc.* **71** (1988) 2071.
68. K. E. GONSALVES, P. R. STRUTT and T. D. XIAAO, *Adv. Mater.* **3** (1991) 202.
69. O. M. GREBZOVA, V. N. TROITSKIY and Y. M. SHULGA, *J. Appl. Chem.* **58** (1985) 2181 (in Russian).
70. G. W. RICE and R. L. WOODIN, *J. Am. Ceram. Soc.* **71** (1988) C. 181.
71. R. A. ANDRIEVSKI, S. E. KRAVCHENKO and S. P. SHILKIN, to be published in *Jap. Jnl. App. Sci.*
72. R. KALYONCU, *Ceram. Eng. Sci. Proc.* **6** (1985) 1356.
73. R. A. ANDRIEVSKI and A. A. NUZHDIN, in "Reviews of Science and Engineering", Powder Metallurgy Series, Vol. 2, edited by L. Trusov (Viniti, Moscow, 1984) p. 3–64 (in Russian).
74. S. J. SAVAGE and O. GRINDER, in "Advances in Powder Metallurgy & Particulate Materials–1992", edited by J. M. Capus and R. M. German (MPIF, Princeton, 1992).
75. I. D. MOROCHOV, L. I, TRUSOV and V. N. LAPOVOK, "Physical Phenomena in Ultradispersed Media" (Energoatomizdat, Moscow, 1984) (in Russian).
76. R. BIRRINGER, U. HERR and H. GLEITER, *Trans. Jpn Inst. Met. Suppl.* **27** (1986) 43.
77. R. W. SIEGEL and H. HAHN, in "Current Trends in Physics of Materials", edited by M. Yussouff (World Scientific Publishing Co., Singapore, 1987) p. 403.
78. H. CHANG, H. J. HOFLER, C. J. ALTSTETTER and R. S. AVERBACK, *Scripta Metall. Mater.* **25** (1991) 1161.
79. G. W. KRIECHBAUM and P. KLEINSCHMIT, *Adv. Mater.* **1** (1989) 330.
80. F. HATAKEYAMA and Sh. KANZAKI, *J. Am. Ceram. Soc.* **73** (1990) 2107.
81. L. HENCH and J. WEST, *Chem. Rev.* **90** (1990) 33.
82. A. E. KRAVCHIK and V. S. NESHPOR, *Powd. Metall.* (1) (1990) 31 (in Russian).
83. V. F. PETRUNIN, Ju. G. ANDREEV, T. N. MILLER and Ja. P. GRABIS, *ibid.* (9) (1987) 90 (in Russian).
84. V. F. PETRUNIN, A. G. ERMOLAEV, A. V. BURCHANOV, E. V. KNIAZEV, L. I. TRUCOV, A. N. ZELIKMAN and S. A. VASILIEV, *ibid.* (3) (1989) 46 (in Russian).
85. E. NEUENSCHWANDER, *J. Less-Common Metals* **11** (1966) 365.
86. S. V. GUROV and V. N. TROITSKIY, in "Plasma-Chemistry-89", edited by L. S. Polak (USSR AS, Moscow, 1989) p. 114 (in Russian).
87. M. I. AIVAZOV, V. V. VOLOD'KO, B. A. EVSEEV and Ju. N. NIKULIN, *Powd. Metall.* (1) (1981) 1 (in Russian).
88. L. I. TRUSOV, V. N. LAPOVOK, V. N. TROITSKIY, E. E. VLASOV, S. B. TERECHOV and T. V. REZCHIKOVA, *Crystallogr.* **27** (1982) 571 (in Russian).
89. S. V. GUROV, V. N. TROITSKIY and A. L. DOROSINSKIY, *Inorg. Mater.* **17** (1981) 431 (in Russian).
90. V. F. PETRUNIN, Yu. G. ANDREEV, T. N. MILLER, Ja. P. GRABIS, A. G. ERMOLAEV and F. M. ZELENIUK, *Powd. Metall.* (8) (1984) 12 (in Russian).
91. S. C. DANFORTH, *Nanostruct. Mater.* **1** (1992) 197.
92. R. A. ANDRIEVSKI, "Particulate Materials Science" (Metallurgia, Moscow, 1991) (in Russian).
93. R. A. ANDRIEVSKI and M. A. LEONTIEV, *Powd. Metall.* (8) (1984) 9 (in Russian).
94. R. A. ANDRIEVSKI, R. A. LUTIKOV and O. D. TORBOVA, to be published in *Inorganic Mtls.*
95. V. I. TORBOV, V. N. TROITSKIY, A. P. ZUEV, V. V. KIREIKO, I. A. DOMASHNEV, V. I. BERESTENKO and O. D. TORBOVA, *Powd. Metall.* (9) (1981) (in Russian).
96. Yu. M. SHULGA, V. N. TROITSKIY, M. I. AIVAZOV and Yu. G. BOROD'KO, *J. Inorg. Chem.* **21** (1976) 2621 (in Russian).
97. Yu. M. SHULGA, G. A. KLJATSHITSKI, V. I. RUBZOV, E. I. KURKIN and V. N. TROITSKIY, *Surface Phys. Chem. Mech.* (9) (1991) 67 (in Russian).
98. Ya. VAIVADS, T. N. MILLER, A. A. KUZYUKEVICH, I. BERTOTI, T. SEKEI and M. LUKACH, *Powd. Metall.* (3) (1990) 80 (in Russian).
99. E. L. NAGAEV, *Usp. Fiz. Nauk* **162** (1992) 50 (in Russian).
100. Ju. M. SCHOENUNG, *Am. Ceram. Soc. Bull.* **70** (1991) 113.
101. R. A. ANDRIEVSKI, S. E. ZEER and M. A. LEONTIEV, in "Physical-Chemistry of Ultradispersed Media", edited by I. V. Tananaev (Nauka, Moscow, 1987) p. 197 (in Russian).
102. R. A. ANDRIEVSKI, *Int. J. Powd. Metall.*, to be published.
103. R. A. ANDRIEVSKI, V. I. TORBOV and E. N. KURKIN, in "Proceedings of the 13th Plansee Seminar '93", Vol 3., edited by H. Bildstein and R. Eck (Metallwerke Plansee, Reutte, 1993) p. 649.
104. S. S. DZHAMAROV, N. P. PAVLENKO, A. V. BOZHKO and P. A. KORNIENKO, *Powd. Metall.* (10) (1982) 6 (in Russian).
105. W. PAN, M. SATO, T. YOSHIDA and K. AKASHI, *Adv. Ceram. Mater.* **3** (1988) 77.
106. W. WAGNER, R. S. AVERBACK, H. HAHN, W. PETRY and A. WIEDENMANN, *J. Mater. Res.* **6** (1991) 2193.
107. V. I. TORBOV, V. N. TROITSKIY and A. Z. RAKHMATULLINA, *Powd. Metall.* (12) (1979) 27 (in Russian).
108. M. MORIYAMA, K. KAMATA and Y. KOBAYASHI, *J. Ceram. Soc. Jpn.* **99** (1991) 286.
109. R. A. ANDRIEVSKI, Yu. S. KONYAEV, M. A. LEONTIEV and G. I. PIVOVAROV, in "High Pressure Research" 1 (Gordon and Beach, London, 1989) p. 329.
110. M. SHIMADA, T. OKAMOTO and M. KOIZUMI, *Mem. Inst. Sci. Ind. Res. Osaka Univ.* **41** (1984) 1.
111. H. OKADA, K. HOMMA and T. FUJIKAWA, *Int. J. Refr. Hard Mater.* **6** (1987) 216.
112. R. A. ANDRIEVSKI, G. M. VOLDMAN and M. A. LEONTIEV, *Inorg. Mater.* **27** (1991) 729 (in Russian).
113. A. S. HELLE, K. E. EASTERLING and M. F. ASHBY, *Acta. Metall.* **33** (1985) 2163.
114. J. SLEURS, R. C. PILLER, M. F. ASHBY and R. W. DAVIDGE, *Silic. Ind.* **57** (1992) 25.
115. R. VASSEN, D. STOVER and H.-P. BUCHKREMER, in "Advances in Powder Metallurgy and Particulate Materials - 1992", edited by J. M. Capus and R. M. German (MPIF, Princeton, 1992).
116. M. D. MATTHEWS and A. PECHENIK, *J. Am. Ceram Soc.* **74** (1991) 1547.
117. H. HAHN and R. S. AVERBACK, *ibid.* **74** (1991) 2918.
118. M. UCHIC, H. J. HOFLER, W. J. FLICK, R. TAO, P. KURATH and R. S. AVERBACK, *Scripta Metall. Mater.* **26** (1992) 885.
119. H. CHANG, H. J. HOFLER, C. J. ALTSTETTER and R. S. AVERBACK, *ibid.* **25** (1991) 1161.
120. P. VERGON, M. ASTIER and S. TEICHNER, in "Sintering and Related Phenomena", edited by G. C. Kuczynski (Plenum Press, New York, 1973) p. 301.
121. G. C. KUCZYNSKI (ed.) "Sintering and Catalysis" (Plenum Press, New York, 1975).
122. R. M. GERMAN, *Sci. Sinter.* **10** (1978) 11.
123. V. N. TROITSKIY, A. Z. RACHMATULLINA, V. I. BERESTENKO and S. V. GUROV, *Powd. Metall.* (1) (1983) 13 (in Russian).
124. R. A. ANDRIEVSKI, M. A. LEONTIEV and A. S. BRAGIN, *Inorg. Mater.* **20** (1984) 2055 (in Russian).
125. R. S. AVERBACK, H. J. HOFLER, H. HAHN and J. C. LOGAS, *Nanostruct. Mater.* **1** (1992) 172.
126. C. XIE, L. ZHANG, Ch. MO, Zh. ZHU, Z. CHEN, Y. QIAN and Y. LI, *J. Appl. Phys.* **72** (1992) 3447.
127. R. A. ANDRIEVSKI, *Sci. Sinter.* **16** (1984) 3.
128. M. A. KUZENKOVA, A. V. KURDUMOV, G. N. MAKARENKO, G. S. OLEINIK and I. G. ROGOVAJA, *Powd. Metall.* (10) (1981) 35 (in Russian).
129. A. V. RAGULJA, ThD, Institute for Materials Science, Ukrainian Academy of Sciences, Kiev (1992) 15p. (in Russian).
130. K. N. P. KUMAR, K. KEIZER, A. J. BURGGRAAF, T. OKUBO, K. NAGAMOTO and Sh. MOROOKA, *Nature* **358** (1992) 48.
131. V. G. GOROBZOV, in "Reviews of Science and Engineering", Powder Metallurgy series, Vol. 5, edited by L. A. Petrova (Viniti, Moscow, 1991) p. 3 (in Russian).

132. K. KONDO, S. SOGA, A. SAWAOKA and M. ARAKI, *J. Mater. Sci.* **20** (1985) 1033.
133. T. TANIGUCHI and K. KONDO, *Adv. Ceram. Mater.* **3** (1988) 399.
134. K. KONDO and S. SAWAI, *J. Am. Ceram. Soc.* **73** (1990) 1983.
135. V. I. KOVTUN and V. I. TREFILOV, *Powd. Metall.* (11) (1989) 85 (in Russian).
136. V. I. KOVTUN, A. V. KURDUMOV, V. B. ZELYAVSKI, N. F. OSTROVSKAYA and V. I. TREFILOV, *ibid.* (12) (1992) 38.
137. T. NISHIDA, H. FUJIOKA, K. ADACHI and K. URABE, *J. Soc. Mater. Sci. Jpn* **41** (1992) 855 (in Japanese).
138. Yu. G. ANDREEV, A. V. BURCHANOV, S. A. BALANKIN, F. MZELENIN, V. F. PETRUNIN, M. V. SCHEPETIN and V. A. JARTSEV, in "Materials Science in Nuclear Engineering" (Moscow Engineering-Physical Institute, Moscow, 1991) p. 72 (in Russian).
139. R. W. SIEGEL and G. J. THOMAS, *Ultramicrosc.* **40** (1992) 376.
140. V. G. GRYAZNOV, M. Yu. TANAKOV and L. I. TRUSOV, *J. Mater. Sci.* **27** (1992) 4829.
141. Y.-M. CHIANG, I. P. SMYTH, C. D. TERWILLIGER, W. T. PETUSKEY and J. A. EASTMAN, *Nanostruct. Mater.* **1** (1992) 235.
142. H. J. HOFLER, H. HAHN and R. S. AVERBACK, Defect Diffus. Forum **75** (1991) 195.
143. A. N. PILYANKEVICH and G. S. OLEINIK, in "High Pressure Influence on Matter", edited by A. N. Pilyankevich (Naukova Dumka, Kiev, 1987) p. 77 (in Russian).
144. G. W. NIEMAN, J. R. WEERTMAN and R. W. SIEGEL, *Nanostruct. Mater.* **1** (1992) 185.
145. R. A. ANDRIEVSKI, in "Advances in Powder Metallurgy and Particulate Materials–1992", edited by J. M. Capus and R. M. German (MPIF, Princeton, NJ, 1992).
146. G. E. FOUGERE, J. R. WEERTMAN, R. W. SIEGEL and S. KIM, *Scripta Metall. Mater.* **26** (1992) 1879.
147. R. A. ANDRIEVSKI, I. A. ANISIMOVA and V. P. ANISIMOV, *Phys. Chem. Mater. Proc.* (2) (1992) 99 (in Russian).
148. D. KIM and K. OKAZAKI, *Mater. Sci. Forum* **88–90** (1992) 553.
149. A. H. CHOKSHI, A. ROSEN, J. KARCH and H. GLEITER, *Scripta Metall. Mater.* **23** (1989) 1679.
150. Z. LI, S. RAMASAMY, H. HAHN and R. W. SIEGEL, *Mater. Lett.* **6** (1988) 195.
151. J. KARCH, R. BIRRINGER and H. GLEITER, *Nature* **330** (1987) 556.
152. F. WAKAI, Y. KODAMA, S. SAKAGUCHI, N. MURAYAMA, K. IZAKI and K. NIIHARA, *ibid.* **344** (1990) 421.
153. R. A. ANDRIEVSKI, *Powd. Metall.* (9) (1992) 1 (in Russian).
154. I.-W. CHEN and Sh. -L. HWANG, *J. Am. Ceram. Soc.* **74** (1992) 1073.
155. M. J. MAJO, R. W. SIEGEL, A. NARAYANASAMY and W. D. NIX, *J. Mater. Res.* **6** (1990) 1073.
156. H. KODAMA and T. MIYOSHI, *J. Am. Ceram. Soc.* **73** (1990) 3081.
157. M. GUERMAZI, H. J. HOFLER, H. HAHN and R. S. AVERBACK, *ibid.* **74** (1991) 2672.
158. H. J. HOFLER and R. S. AVERBACK, *Scripta Metall Mater.* **24** (1990) 2401.
159. A. SAWAGUCHI, K. TODA and K. NIIHARA, *J. Am. Ceram. Soc.* **74** (1991) 1142.
160. N. NIIHARA, K. IZAKI and T. KAWAKAMI, *J. Mater. Sci. Lett.* **10** (1990) 112.
161. N. G. ASKUNTOVICH, R. P. BOROVIKOVA, L. I. TRUSOV, V. N. LAPOVOK and R. G. MIKELADZE, *Solid State Phys.* **27** (1982) 3152 (in Russian).
162. *Idem, ibid.* **27** (1982) 3154 (in Russian).
163. L. I. TRUSOV, N. G. ASKUNTOVICH, R. P. BOROVIKOVA, M. A. BAKLASTOV and V. P. FEDOTOV, *Phys. Lett. A.* **167** (1992) 306.
164. O. L. DOZHDIKOVA, Yu. P. ZARICHNYAK, A. V. ZUEV, S. O. KRYLOV, S. S. ORDANIYAN and E. K. STEPANENKO, *Powd. Metall.* (5) (1992) 70 (in Russian).
165. I. A. DOMASHNEV, in "Dispersed Powders and Materials on Their Base", edited by V. V. Skorochod (Ukranian Academia of Sciences, Kiev, 1982) p. 167.
166. V. N. TROITSKIY, I. A. DOMASHNEV, E. N. KURKIN, O. M. GREBZOVA, O. M. GREBZOVA, A. A. BUDANOV, S. V. GUROV and G. Ja. KLIASCHIZKIY, *Chem. High Energy* **27** (1993) to be published in *Chemistry of High Energy* (in Russian).
167. R. A. ANDRIEVSKI, *Mendeleev Chem. J.* **36** (2) (1991) 11.
168. R. A. ANDRIEVSKI and I. A. ANISIMOVA, *Inorg. Mater.* **27** (1991) 1450 (in Russian).
169. I. N. FRANTSEVICH, S. N. GROMYKO, A. N. KURDUMOV, V. M. MELNIK and G. S. OLEINIK, in "Superhard Materials: Synthesis, Properties, and Applications", edited by I. N. Frantsevich (Naukova Dumka, Kiev, 1983) p. 24 (in Russian).
170. O. N. GRIGOR'EV, V. I. TREFILOV and A. M. SHATOKHIN, *Powd. Metall.* (12) (1983) 75 (in Russian).
171. *Int. J. Refr. Hard Metals* **6** (1987) 180.
172. R. BOHN, T. HAUBOLD, R. BIRRINGER and H. GLEITER, *Scripta Metall. Mater.* **25** (1991) 811.
173. *Powd. Metall. Int.* **24** (1992) 368.

Received 25 March
and accepted 5 May 1993